Evaluation of SMA-RL71, a curcumin analogue nanomicelle as a drug in xenograft models of triple negative breast cancer

Vignesh Sundararajan

A thesis submitted for the degree of
Master of Science in Pharmacology
at the University of Otago, Dunedin,
New Zealand.

Date of submission: 26th June 2014

Abstract

Triple negative breast cancer (TNBC) is a subtype of ER (-) cancer that currently has no treatment options. A novel drug formulation of the most potent curcumin analogue (RL71), compared to the analogues synthesised by other laboratories, styrene-co-maleic acid - 3,5-bis (3,4,5-trimethoxybenzylidene)-1 methylpiperidin-4-one (SMA-RL71) was tested for its anti-cancer activity in an animal model of breast cancer. In the dose response study 15 mg/kg, 10 mg/kg and 5 mg/kg of SMA-RL71 and 10 mg/kg of RL71 was injected into the tail vein of female SCID mice inoculated with MDA-MB-231 cells. None of the treatments produced a statistically significant decrease in tumour volume. Since SMA-RL71 15 mg/kg caused necrosis of the tail, a time course study was performed using SMA-RL71 10 mg/kg at different time points to test if tumour suppression could be achieved with multiple injections of the drug. Mice were randomly grouped after tumour inoculation and dosed with SMA-RL71 10 mg/kg (2 weeks), SMA-RL71 10 mg/kg (3 weeks), RL71 10 mg/kg (2 weeks), and RL71 10 mg/kg (3 weeks) via the tail vein, twice weekly (every 3-4 days). Tumour volume and body weight were determined twice weekly and tumour weight was determined at necropsy. Toxicity was determined from the organ weight at the time of necropsy. Compared to control, there was a 46% decrease ($P < 0.001$) in tumour volume in the mice dosed with SMA-RL71 10 mg/kg for 2 weeks from day 24. Furthermore, on day 31 when the mice were sacrificed, there was a 43% decrease ($P < 0.0001$) in tumour weight. All mice gained a similar amount of weight at the end of each study. However, an increase in the weight of the spleen, liver and kidney were observed in the mice dosed with SMA-RL71. HPLC was optimised for the detection of RL71 in plasma, using curcumin as an internal standard. In summary, 15% SMA-RL71 10 mg/kg twice weekly for two weeks suppressed the growth of TNBC tumours without any significant loss in body weight.

Acknowledgements

I would like to thank Assoc. Prof. Rhonda J. Rosengren and Dr. Khaled Greish for their help in planning and executing my project. Their encouragement, constant input and suggestions to solve the problems helped me to a great extent. I would also like to thank Dr. Sebastien Taurin for teaching me the techniques and helping with the various aspects of my project. I would also like to thank my other supervisor, Dr. Bill Hawkins, from the Department of Chemistry for his suggestions in solving the issues with HPLC.

Thanks also to Dr. Floriane Imhoff, Dr. Belinda Cridge, and Mhairi for explaining and helping me with cell culture experiments.

Special thanks to Rob for bringing HPLC back to life at a stage when I had no hope of successfully optimising it. Your help, ideas and encouragement greatly boosted my confidence to work with HPLC. Thanks also to Mhairi for her help.

Thank you to all the students in the lab – Patrick, Hannah and Tara. Thanks to Hannah and Patrick for helping me whenever I needed. Your help is greatly appreciated. Thanks to Neha for explaining me the concepts of HPLC. Thanks also to Vishal and Sweta for helping me when I needed so desperately.

Thank you also to my family and friends for their constant support.

Finally, thanks to everyone else who may have helped me.

Table of Contents

Chapter Three: Results

Chapter Four: Discussion

List of Figures

List of Tables

List of Abbreviations

Akt serine/threonine – specific protein kinase family or protein kinase B

ALT alanine transaminase

AUC area under the curve

BMHPC 2,6-bis((3-methoxy-4-hydroxyphenyl)methylene)-cyclohexanone

BRCA1 breast cancer gene 1 that acts as a tumour suppressor gene

BSA bovine serum albumin

CDK cyclin dependent kinase

CD105 type I membrane glycoprotein located on cell surface and part of TGFβ receptor complex. Also known as endoglin.

CK cytokeratin

Compound B02 (1E,4E)-1,5-Bis(3-hydroxy-2-methoxyphenyl)penta-1,4-dien-3-one

Compound B33 (1E,4E)-1,5-Bis(2-bromophenyl)penta-1,4-dien-3-one

Compound 15H (1E,4E)-1-(5-hydroxy-1-methyl-1H-benzo[d]imidazol-2-yl)-5-(3-hydroxy-4-methoxyphenyl)penta-1,4-dien-3-one

Compound 18 3,5-bis(4-hydroxy-3-methoxy-5-methylcinnamyl)-*N*-ethylpiperidone

COX-2 cyclooxygenase-2

Cur-OEG curcumin oligo ethylene glycol nanoparticles

DBM dibenzoylmethane

DMBA 7, 12-dimethylbenz[a]anthracene

DMEM/Ham F12 dulbecco's modified eagle's media/nutrient mixture F-12 Ham

DMSO dimethyl sulfoxide

DNA deoxyribonucleic acid

EDAC N-(3-dimethylaminopropyl)-N-ethyl- carbodiimide hydrochloride

EDTA ethylenediaminetetraacetic acid

EF24 (3, 5-Bis-(2-fluorobenzylidene)-piperidin-4-one, acetic acid salt)

EGF epidermal growth factor

EGFR epidermal growth factor receptor

EPR enhanced permeability and retention

ER oestrogen receptor

ERK extracellular signal-regulated kinase

FBS foetal bovine serum

fVIIa coagulation factor VIIa

GSH glutathione

GST glutathione S-transferase

HC hydrazinocurcumin

HCl hydrochloric acid

Her2 human epidermal growth factor receptor-2

H & E haematoxylin and eosin

HIF-1 hypoxia inducible transcription factor-1

HPLC high performance liquid chromatography

HUVEC human umbilical vascular endothelial cell

IC_{50} concentration that kills 50% of cells

i.duc. intraductally (route of administration)

IFN-γ interferon gamma

IHC immunohistochemistry

IL-2 interleukin-2

IL-10 interleukin-10

IL-12 interleukin-12

i.p. intraperitoneal (route of administration)

i.v. intravenous (route of administration)

JAK janus kinase

JNK c-Jun N-terminal kinase

kDA kilo Dalton

LAK lymphocyte-activated killer cells

LOD limit of detection

LOQ limit of quantitation

MAPK mitogen-activated protein kinase

MEM minimum essential medium

MMP-2 matrix metalloproteinase-2

MMP-9 matrix metalloproteinase-9

MNU N-methyl-N-nitrosourea

MPA medroxyprogesterone acetate

MRI magnetic resonance imaging

MTD maximum tolerated dose

mTOR mammalian target of rapamycin

MVD microvessel density

NaCl sodium chloride

$NaHCO_3$ sodium hydrogen carbonate

NFκB nuclear factor kappa-light-chain-enhancer of activated B cells

NO nitric oxide

OCT optimal cutting temperature compound

OEG oligo (ethylene glycol)

Oestrogen 17β-oestradiol

PAC 5-bis (4-hydroxy-3-methoxybenzylidene)-N-methyl-4-piperidone

PARP poly ADP-ribose polymerase

PBS phosphate buffered saline

PEG polyethylene glycol

PKA protein kinase A

PLGA poly (lactic-co-glycolide)

PR progesterone receptor

pSTAT3 phosphorylated signal transducers and activators of transcription-3

RES reticulo-endothelial system

RL66 3,5-bis (pyridine-4-yl)-1-methylpiperidin-4-one

RL71 3,5-bis (3,4,5-trimethoxybenzylidene)-1 methylpiperidin-4-one

RL90 2, 6-bis (pyridin-3-ylmethylene)-cyclohexanone

RL91 2, 6-bis (pyridin-4-ylmethylene)-cyclohexanone

ROS reactive oxygen species

SCID severe combined immunodeficiency

SEM standard error of mean

SF silk-fibroin

SMA styrene-co-maleic acid

SNR signal-to-noise-ratio

SPF s-phase fraction

STAT signal transducers and activators of transcription

TGF-β transforming growth facot-beta

TIMP tissue inhibitor of metalloproteinases

TNBC triple negative breast cancer

Tris-HCl Tris[hydroxymethyl]aminomethane hydrochloride

VEGF vascular endothelial growth factor

VHL von hippel landau

Master of Science thesis
Vignesh Sundararajan
'Evaluation of SMA-RL71, a curcumin analogue nanomicelle as a drug in xenograft models of triple negative breast cancer.'

Response Sheet

- Source of plasma for HPLC: Control mouse plasma.

- Other methods were not trialled to improve recovery. The work performed was at its preliminary stage where the foremost goal was to test if the method for plasma extraction optimised by Dr. Lesley Larsen in gradient mode would work without causing any interference with the peak of interest using the new mobile phase. Further work would have been to test if reproducibility was achieved, and then explore the possibilities of using other chemicals along with or without methanol to improve the recovery.

- The injection volume was chosen as 10 µL because it was observed during method development that increasing the amount of injection volume, such as 60 or 70 µL, resulted in a peak resembling a bell-shaped curve.

- HPLC method used by Yadav *et al:* Mobile phase was acetonitrile in water with 0.1% formic acid in gradient mode for 20 minutes. The flow rate was 0.3 mL/min and the injection volume 5 µL.

- Surrogate for plasma extraction: RL116 was used as a surrogate because of its similarity to the compound of interest (RL71). Moreover, recovery from a surrogate can also be used to assess instrument performance and extraction efficiency of the compound of interest [1, 2, and 3].

- Yes, doubling the volume of injection will halve the LOD and LOQ.

- The precision and accuracy of the assay by HPLC was monitored by:

  a) Plotting standard curves multiple times during a single run, at different times, to assess if reproducibility was achieved.
  b) Using check standards throughout an analytical run.
  c) Running each sample at least 3 times.
  d) Comparing standard curves from the same standards run at different times.

- During micelle preparation, the pH was reduced to 3 by adding 1 M HCl to precipitate the micelles. The solution was then centrifuged at 3,000 rpm for 5 min and the supernatant discarded. The pellet was dissolved in MilliQ water and the pH raised to 7.4 using 0.1 N NaOH. The rationale behind decreasing the pH to 3 and centrifuging it was to remove any free drug that was not encapsulated in the micelle.

- Different vehicles were used in each study because different solutions were used to solubilise the micelle.

- Normalised tumour volume is the ratio of tumour volume to its corresponding control value, multiplied by 100. This was used since all points in the graph would have the same tumour volume on day one.

- The various mechanisms described for drug resistance are only possibilities; there is no evidence to state that they are the exact cause. To investigate if the drug was detoxified by conjugation with glutathione, it is suggested to perform glutathione – S - transferase (GST) activity assay. Briefly, this involves preparation of lysate from the tumours and incubating a known amount of the lysate with 1 –chloro-2, 4, dinitrobenzene substrate and L-glutathione. The rate of conjugation of the substrate to glutathione by GST should then be measured, which will help in the determination of total GST activity [4].

- Treatment of MDA-MB-231 cells with RL71 did decrease the expression of NFκB at 24 h and 36 h post-treatment. However, in a study by Montagut *et al*., it was found that NFκB was also activated after treatment with chemotherapeutic agents such as taxane, which significantly (85%) contributed to chemoresistance. This was confirmed by nuclear staining of NFκB from tumour specimens obtained from breast cancer patients post –treatment. The authors do mention the fact that addition of NFκB inhibitors might help in overcoming its activation [5]. However, in the present study, multiple injections of the drug was used at different time points. There is no evidence at this stage to state that NFκB activation led to decreased response in the 3-weeks treated group. Nevertheless, NFκB activation is one of the most common reasons for drug resistance, and it is only a possibility that beyond a threshold limit, the drug becomes less effective in NFκB inhibition.

[1] Volz, S. A.; Johnston, J.J.; and Griffin, D.L., "Solid Phase Extraction Gas Chromatography/Electron Capture Detector Method for the Determination of Organochlorine Pesticides in Wildlife Whole Blood" (2001). USDA National Wildlife Research Center - Staff Publications. Paper 574.

[2] Marquardt, R., Meng, M., Brough, R., Bennett, P.K., Chou, B., Rudewicz, P., "Quantification of Endogenous Plasma Thymidine Using 13C Labeled Thymidine As Surrogate Analyte" (2007). ASMS 55th Conference on Mass Spectrometry, Indianapolis, Indiana, June 2007. Retrieved from http://www.tandemlabs.com/documents/ASMS_07_Min_Web.pdf.

[3] Gupta, P.K., Brown, J., Biju, P.G., Thaden, J., Deutz, N.E., Kumar, S., Hauer-Jensen, M., Hendrickson, H.P., (2011) "Development of high-throughput HILIC-MS/MS methodology for plasmacitrulline determination in multiple species." *Analytical Methods*, 3, 1759.

[4] LaPensee E.W., Schwemberger S.J., LaPensee C.R., Bahassi el M., Afton S.E., Ben-Jonathan N., (2009). “Prolactin confers resistance against cisplatin in breast cancer cells by activating glutathione-S-transferase.” *Carcinogenesis* 30(8), 1298-1304.

[5] Montagut, C., Tusquets, I., Ferrer, B., Corominas, J.M., Bellosillo, B., Campas, C., Suarez, M., Fabregat, X., Campo, E., Gascon, P., Serrano, S., Fernandez, P.L., Rovira, A. and Albanell, J. (2006). "Activation of nuclear factor-kappa B is linked to resistance to neoadjuvant chemotherapy in breast cancer patients." *Endocrine-Related Cancer,* 13(2): 607-616.

Chapter One: Introduction

1.1 Breast Cancer

1.1.1 Breast Cancer Incidence

Breast cancer is estimated to be the most frequently diagnosed cancer in women, contributing to 16% of all female cancers and is also one of the major causes of death worldwide (Liang *et al*., 2010). In New Zealand, it is the most commonly diagnosed cancer among women, contributing to approximately 2600 new cases every year (New Zealand Breast Cancer Foundation, 2011). The incidence of breast cancer in New Zealand women is high, with one in nine chance of developing the disease. The risk also increases with age (New Zealand Breast Cancer Foundation, 2011).

1.1.2 Classification

Breast cancer can be broadly classified as either oestrogen receptor positive (ER +) or oestrogen receptor negative (ER -) (Petrangeli *et al.*, 1994, Robertson, 1996). The most common form of breast cancer is invasive ductal carcinoma, contributing to 85% of all breast cancer cases (Liang *et al*., 2010). The conventional prognostic markers predicting the overall survival include tumour volume, tumour grade, and axillary lymph node status (Pervez *et al.*, 2007). Some of the newer markers include DNA ploidy, S-phase fraction (SPF), p53, human epidermal growth factor receptor-2 (Her2), and EGFR (Pervez *et al.*, 2007). Sub-classification of invasive ductal carcinoma is based on the immunostaining of tumour tissues for ER, progesterone receptor (PR), and Her2 (Sandhu *et al.*, 2010). Tumours lacking the expression of these receptors are referred to as 'triple negative breast cancer' (TNBC) (Sandhu *et al.*, 2010). As breast cancer is a heterogeneous disease, a more descriptive classification based on gene - expression profiling of tumours is used to classify it into five major groups: luminal A, luminal B, normal breast-like, Her2 overexpression, and basal-like (Rhee *et al.*, 2008). The term triple negative breast cancer is frequently used for the basal-like tumours as 80-90% of the triple negative tumours have the characteristics of basal-like type (Rhee *et al.*, 2008). Table 1 summarises the breast cancer subtypes and their characteristics.

The triple negative tumours are difficult to treat (Liedtke *et al.*, 2008) and are characterised by relapse within three years with poor survival rates, especially in the first three years of post-recurrence (Liedtke *et al.*, 2008, Zhang *et al.*, 2013). The standard treatment for patients with TNBC is cytotoxic chemotherapy (Rowe *et al.*, 2009). The most common immunohistochemical and gene expression changes in TNBC include *p53* and BRCA1 mutations, overexpression of EGFR, caveolin-1, P-cadherin, basal cytokeratins (CK5, CK17), and Ki67 (Schneider *et al.*, 2008). Because the triple negative tumours express neither ER, PR nor Her2, they are highly resistant to some of the drugs used to treat breast cancer (Stuart *et al.*, 2010). Though TNBC accounts for a minority of the breast cancers, they have high mortality rates due to their aggressive nature and lack of targeted therapies (Duffy *et al.*, 2012). Compared to other types of cancers, TNBC has a younger

mean age of diagnosis (Dent *et al.*, 2007). Patients diagnosed with TNBC are more likely to have a larger tumour volume and a grade III tumour (Dent *et al.*, 2007). The majority of TNBC patients have distant recurrence and the median survival rate is 4.2 years (Dent *et al.*, 2007). TNBC is more frequently seen in women of African and Hispanic ancestry. Visceral metastasis is more commonly seen with TNBC, with the lungs and brain being the most common sites of metastasis, and bone metastasis is seen only rarely (Kennecke *et al.*, 2010, Hudis and Gianni, 2011, Criscitiello *et al.*, 2012).

Table 1: Summary of breast cancer subtypes and their characteristics (Sørlie *et al.*, 2001, Rakha *et al.*, 2008, Rhee *et al.*, 2008, Sandhu *et al.*, 2010, Tran and Bedard, 2011).

Breast cancer subtype	Characteristics
Luminal A	ER (+), with high levels of ER expression. These tumours have a better prognosis.
Luminal B	ER (+). Comparatively low levels of ER expression and overexpression of Her2. Increased expression of proliferation genes such as CCNB1, MKI67 and MYBL2. Compared with luminal A tumours, these have a poor prognosis.
Her2 overexpression	ER (-), PR (-), and Her2 (+). Comparatively better survival rates because of the ability to target them using herceptin.
Normal breast-like	ER (-). Characterised by their resemblance to normal breast tissue with elevated expression of genes associated with adipose cells, other non-epithelial cells and low expression of genes associated with luminal epithelial cells.
Basal-like (Triple Negative cancer)	Lack ER, PR, and Her2. Very aggressive, difficult to treat, and associated with poor prognosis. Characterised by the expression of genes associated with basal epithelial cells.

1.2 Curcumin

Curcumin or diferuloylmethane, a phenolic compound extracted from the roots of *Curcuma longa,* has been used widely as a colouring agent, food additive and in Indian traditional medicine (Sandur *et al.*, 2007). It possesses antioxidant, anti-inflammatory, and anti-cancer properties (Sandur *et al.*, 2007). The constituents of curcumin available commercially are 77% curcumin, 18% demethoxycurcumin, and 5% bisdemethoxycurcumin (Sandur *et al.*, 2007). Curcumin has been used as an anti-

inflammatory agent due to its ability to block nuclear factor-kappaB (NFκB) activation (Aggarwal and Harikumar, 2009). In tumour cells, it inhibits various proteins that control proliferation, invasion and angiogenesis (Aggarwal and Harikumar, 2009). Because of its anti-inflammatory properties, curcumin has been used against neurodegenerative, cardiovascular, pulmonary, metabolic, and autoimmune diseases (Aggarwal and Harikumar, 2009).

In various cancer models, curcumin elicits anti-inflammatory action by inhibiting cyclooxygenase-2, lipoxygenase, and inducible nitric oxygenase (Brouet and Ohshima, 1995, Menon and Sudheer, 2007). At the molecular level, curcumin interacts with a wide variety of target molecules. Some of the target molecules are enzymes such as haem oxygenase-I (Balogun *et al.*, 2003), Ca(2+)-ATPase (Logan-Smith *et al.*, 2001), and Na,K-ATPase (Mahmmoud, 2005), telomerase, glutathione S-transferase (GST), transcription factors such as NFκB, Notch-1, signal transducers and activators of transcription (STAT), and β-catenin (Review: Grynkiewicz and Slifirski, 2012), protein kinases such as mitogen-activated protein kinase (MAPK) (Lee *et al.*, 2009), janus kinase (JAK), and protein kinase A (PKA) (Review: Grynkiewicz and Slifirski, 2012), receptors such as oestrogen receptor-α (ER-α), Her2, and epidermal growth factor receptor (EGFR) (Review: Grynkiewicz and Slifirski, 2012) and anti-apoptotic proteins such as bcl-2 (Lee *et al.*, 2009). Curcumin also inhibits chemical-induced carcinogenesis at the initiation and progression stages (Thangapazham *et al.*, 2006) and the bioactivation of environmental carcinogens such as benzo[a]pyrene by acting as a competitive inhibitor of cytochrome P450A1 (Singh *et al.*, 1998). Furthermore, by inducing haem oxygenase-1 via the activation of the transcription factor Nrf2, curcumin protects the body from various forms of stress (Balogun *et al.*, 2003).

Several studies show that curcumin has potent anti-cancer activity against different types of breast cancer cell lines and in animal models (Verma *et al.*, 1997, Shao *et al.*, 2002, Bachmeier *et al.*, 2007, Carroll *et al.*, 2010, Lai *et al.*, 2012, Jiang *et al.*, 2013, Masuelli *et al.*, 2013).

1.3 Problems Associated with Curcumin

1.3.1 Pharmacokinetics

Though curcumin has shown great potential as an anti-cancer agent in several cancer models, inherent problems associated with it such as poor absorption, rapid metabolism, and water insolubility have hindered its successful development as a chemotherapeutic agent.

An *ex-vivo* study using everted rat intestinal sacs incubated with curcumin (50-750 µg) showed that the compound had poor intestinal absorption. Approximately 30-80% of curcumin was lost from the mucosal side, with only less than 3 % being found in the tissue. The serosal fluid did not show any presence of curcumin. The authors also reported the

transformation of the compound during intestinal absorption (Ravindranath and Chandrasekhara, 1981).

The fate of curcumin in rats was studied using Sprague-Dawley rats. Rats of both sexes were orally gavaged with curcumin (1 g/kg) dissolved in arachis oil. Three days after the oral dosage, excretion via the faecal route accounted for 65-85% of loss. The maximum elimination was observed at 48 h. Curcumin was detectable in plasma 3 h after injection, but was beyond the limit of detection at 6 h. However, when injected intravenously, curcumin was cleared rapidly and was beyond the limit of detection within an hour. These results show that curcumin has a very low absorption and is also rapidly metabolised (Wahlström and Blennow, 1978). Another study also showed that curcumin administered orally at a dose of 2 g/kg to rats produced a maximum serum concentration at 0.83 h; serum levels of curcumin were also low in humans when administered a dose of 2 g, even at 1 h after dosing. Supplementing curcumin with piperine to inhibit glucuronidation resulted in a significant improvement in bioavailability and absorption (Shoba *et al.*, 1998).

The pharmacokinetic properties of curcumin when given orally versus intraperitoneally (i.p.) in mice produced a completely contrasting result. With oral administration of 1 g/kg, the maximum concentration in plasma (0.22 µg/ml) was detected at 1 h, and was below the limit of detection within 6 h (5 ng/ml). However, when dosed intraperitoneally, the concentration was much higher in plasma at 15 min (2.25 µg/ml), which rapidly declined within an hour (Pan *et al.*, 1999). Tissue distribution studies with curcumin in orally gavaged rats show that 0.015% of the administered curcumin deposited in the liver, kidneys, and body fat after 3 h and small intestine had the maximum accumulation. Liver perfusion studies also demonstrated that 49 % of the curcumin was excreted as glucuronide conjugate, and also as conjugated sulphate (Wahlström and Blennow, 1978, Ravindranath and Chandrasekhara, 1980). Studies investigating curcumin conjugation show that the enzyme responsible for such reactions are mainly located in liver, kidney and intestinal mucosa (Asai and Miyazawa, 2000). Intravenous injection of curcumin in rats and liver perfusion experiments show the accumulation of the compound in liver and kidney, with the liver being the major site of metabolism (Wahlström and Blennow, 1978). Some groups have used radioactive curcumin to trace the metabolism and elimination of curcumin after dosing. For this, mice were dosed with [^{14}C] curcumin (100 mg/kg) intraperitoneally and the radioactivity in different organs was measured. Intestinal mucosa had the highest radioactivity, followed by kidney, liver and plasma. Negligible amounts were found in brain, heart, lungs and muscle. After 4 h, the peak values reduced to 20-33% of the initial values (Perkins *et al.*, 2002).

1.3.2 Bioavailability

Another factor that contributes to the low bioavailability of curcumin is its clearance from the body. Shoba *et al.* studied the pharmacokinetics of curcumin in rats and human volunteers. Rats orally administered with curcumin 2 g/kg had an absorption half-life of 0.31 ± 0.07 h and an elimination half-life of 1.7 ± 0.5 h. The same dose in humans was beyond the limit of detection in serum (Shoba *et al.*, 1998). Yang *et al.* studied the oral

bioavailability of curcumin in rat using tandem mass spectrometry. Oral administration of curcumin (500 mg/kg) resulted in an elimination half-life of 28.1 ± 5.6 min, whereas i.v injection of curcumin (10 mg/kg) resulted in an elimination half-life of 44.5 ± 7.5 min (Yang *et al.*, 2007).

Aqueous solubility of curcumin is also a major factor contributing to its low bioavailability and reduced pharmacological benefits. Curcumin is hydrophobic and water insoluble, but soluble in organic solvents such as methanol (Kurien *et al.*, 2007). Curcumin undergoes hydrolytic degradative reactions in aqueous solutions. At pH below 7, it is stable but aqueous solubility is poor. Without a stabilising agent, curcumin is very unstable in aqueous solutions at pH >7. Under alkaline conditions, the hydrolytic degradation products formed are feruloyl methane, ferulic acid and vanillin. In organic solvents, curcumin also undergoes photodegradation. (Tønnesen and Karlsen, 1985, Tønnesen *et al.*, 2002).

All these factors greatly affect the efficacy and targeted delivery of curcumin in animal models and clinical studies. Owing to its low bioavailability and rapid elimination from the systemic circulation, high doses of curcumin are required to achieve accumulation in tumours and significant results in clinical trials. Hence, nanoparticle formulation of curcumin is currently being tested.

1.4 Novel Drug Delivery of Curcumin

Owing to the poor bioavailability and rapid metabolism of curcumin, nanotechnology has been used to improve the efficacy of curcumin. Some of the commonly used nanotechnology approaches include nanoparticles, liposomes, micelles, and phospholipid complexes. All these novel approaches improved the absorption and biodistribution. The nano forms are more effective than curcumin because of their physiochemical properties (Anand *et al.*, 2008). Nanocurcumin has several advantages such as better solubilisation, tumour-specific accumulation, high stability, reduced clearance from the body, and controlled release (Figure 1). These features make it a better candidate than curcumin (Yallapu *et al.*, 2013).

A study in rats intravenously administered with curcumin and nanocurcumin showed that nanocurcumin had greater tissue distribution in different organs due to increased half-life and mean residence time. Curcumin was mainly found in liver and kidneys, where it was metabolised and eliminated from the body. This significantly decreased the systemic circulation of curcumin. However, nanocurcumin was found mainly in the spleen and lungs, and very little in the metabolising organs and heart. Both curcumin and nanocurcumin crossed the blood-brain barrier, but the nanoformulation had better biodistribution in brain compared to curcumin. Overall, the authors concluded that the nanosized formulation resulted in a better biodistribution pattern (Tsai *et al.*, 2011).

Another advantage of nanocurcumin is that it provides controlled release of drug. It also demonstrated better uptake and efficacy in breast cancer cells. This led to overall improvements in the retention, efficacy, and bioavailability of curcumin (Gupta *et al.*, 2009). Nanocurcumin was also more soluble than curcumin, as curcumin-loaded PLGA

nanospheres were completely soluble in aqueous media without any aggregate formation (Mukerjee and Vishwanatha, 2009). Also, using inert hydrophilic polymers such as poly(ethylene glycol) and poly(vinyl alcohol) can help in overcoming opsonisation and non-specific accumulation of nanoparticles in organs (Yallapu *et al.*, 2010). Nanocurcumin is a superior drug carrier with a loading capacity up to 25 wt/wt% and encapsulation efficiency of 70-90%. Thus, controlled release of curcumin from nanoparticles dramatically improves the accumulation of curcumin in tumours (Yallapu *et al.*, 2013). In animal models, curcumin nanoparticles greatly enhanced the accumulation of curcumin in tumour tissues, resulting in increased number of apoptotic cells and decreased cell proliferation (Liu *et al.*, 2013).

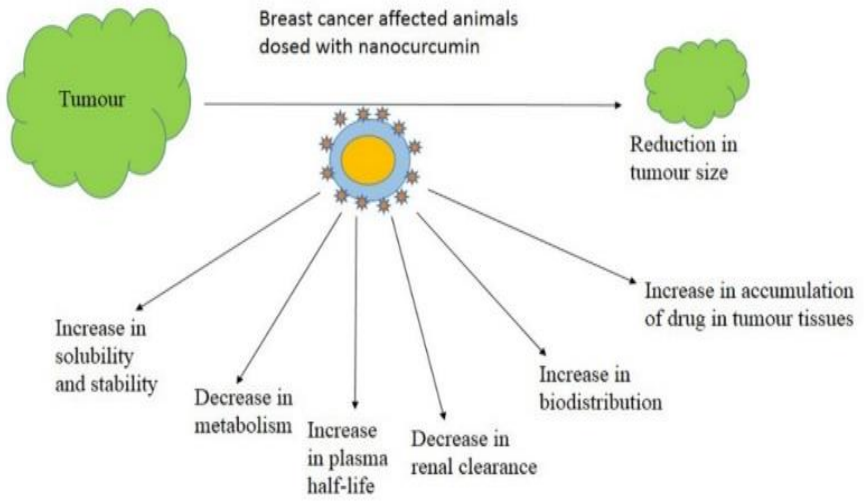

Figure 1: Schematic representation of the factors involved in tumour suppression by nanocurcumin/ nanoformulation of curcumin analogues.

1.5 The EPR Effect

The concept of using nanomedicine to deliver drugs selectively to the tumour tissue is based on the phenomenon of 'enhanced permeability and retention' (EPR) effect (Greish, 2007, Iyer *et al.*, 2007), first described by Maeda *et al*. in 1985 while working towards improving the pharmacological properties of the anti-cancer drug neocarzinostatin by conjugating it to styrene-co-maleic acid (SMA) (Maeda *et al.*, 1985). This phenomenon makes use of the abnormal vasculature of the tumour tissues. Tumour tissues are characterised by irregularly shaped, dilated, highly permeable, and leaky blood vessels with large pores (Yuan, 1998, Greish, 2007). The endothelial cells of the tumour blood vessels have wide fenestrations, lack a smooth muscle layer, and functional receptors for angiotensin II (AT-II) (Fang *et al.*, 2011). They also have defective lymphatic drainage in that the macromolecules are not cleared effectively from the interstitial space (Noguchi *et al.*, 1998). Vascular mediators such as bradykinin, nitric oxide (NO), and prostaglandins

also contribute to the enhanced permeability of the tumour tissues (Wu *et al.*, 1998). The submicron size of the nanoparticle also helps in its selective accumulation in tumour tissue. The nanoconstructs must range in size from approximately 10 to 100 nm to utilise the EPR effect. Those smaller than 10 nm by cleared by the kidneys and those ranging from approximately 100-200 nm are cleared by the reticulo-endothelial system (RES) (Petros and DeSimone, 2010). The molecular weight of the drug plays an important role in its ability to accumulate in tumour tissues. Nanoparticles larger than 40 kDa have a longer circulation time and a reduced clearance rate from the body (Fang *et al.*, 2011). Neutrally-charged molecules circulate in the blood longer than the negatively and positively-charged ones, which are eliminated rapidly by the phagocytic cells of the liver (Li and Huang, 2008, Arnida *et al.*, 2011). Surface modification using polyethylene glycol (PEG) and its derivatives reduces the negative charge and prevents rapid clearance of the drug by RES (Moghimi *et al.*, 2001, Li and Huang, 2008). Taken together, all these factors help in selective accumulation of nanodrugs in tumour tissues.

1.6 Nanocurcumin – in vitro and *in vivo* effects

Gupta *et al.* studied the effect of silk-fibroin (SF) derived curcumin nanoparticles in MDA-MB-453 breast cancer cells, which have a high expression of Her2. SF nanoparticles with 10% SF coating and less than 100 nm in size had better uptake, efficacy, and release rate (Gupta *et al.*, 2009). Curcumin, when encapsulated in poly (lactic-co-glycolide) (PLGA), a biodegradable polymer, showed a six-fold increase in uptake in triple negative MDA-MB-231 breast cancer cells. The nanocurcumin was superior to free curcumin with an IC_{50} value of 9.1 µM in MDA-MB-231 cells. The nano form elicited concentration-dependent anti-proliferative effects and inhibited colony formation with just 40% release of the drug from the polymer. It also caused an 8-fold increase in the number of apoptotic cells (Yallapu *et al.*, 2010).

In another approach, curcumin was conjugated with oligo (ethylene glycol) to form Cur-OEG nanoparticles. It elicited apoptosis in several cancer cell lines and reduced tumour volume in a MDA-MB-468 xenograft model. The nanoparticle also did not cause acute or chronic toxicity when dosed with 100 or 250 mg/kg (Tang *et al.*, 2010). In an *in vivo* study using MDA-MB-231 xenografts, a single dose of PLGA-curcumin nanoparticles injected subcutaneously in mice demonstrated sustained release of the drug, with much higher accumulations in metastatic sites such as lungs and brain. The nanoparticle also reduced the tumour volume by 49%, compared to empty nanoparticle-treated mice, by down-regulating the expression of markers of angiogenesis, metastasis and proliferation such as VEGF, MMP-9, Ki-67, and cyclin D1. The nanoparticle treated tumours also had much smaller and poorly developed CD31 positive microvessels. Interestingly, in the same study, repeated systemic administration of curcumin (4.4 mg, intraperitoneally) did not result in inhibition of tumour growth (Shahani *et al.*, 2010).

Chun *et al.* studied the effect of NanoCurc, curcumin encapsulated in a polymer composed of N-isopropylacrylamide, vinylpyrrolidone and acrylic acid in female Sprague–Dawley rats injected with N-methyl-N-nitrosourea (MNU) to induce breast cancer. Two different

experiments were performed. In the first study, MNU-rats were administered either NanoCurc dissolved in phosphate-buffered saline or an empty nanoparticle in PBS. The NanoCurc delivered approximately 168 µg of curcumin per teat. Two intraductal (i.duc) injections were given, the first on day 14 post-MNU exposure and the next 4 weeks after the first injection. Rats were then observed for 34 weeks post-MNU exposure for tumour incidence. While the rats treated with empty nanoparticles had a tumour incidence of 22%, the NanoCurc-treated rats had a tumour incidence of 8%. In the second study, the rats were randomised into four groups and were administered either oral free curcumin (200 mg/kg), i.duc free curcumin, i.duc NanoCurc (168 µg of curcumin) or i.duc empty polymer. Three treatments were given. The first one was at day 14 post-MNU exposure. The other two treatments were at 7 and 14 days following the first injection. The rats were observed for 24 weeks post-MNU exposure for the presence of palpable tumours. Among the treatment groups, the i.duc NanoCurc rats had the smallest mean tumour volume (1672.7 mm^3). This was associated with a decrease in NFκB (approximately 84%), and proliferation marker Ki67 (approximately 93% decrease). Interestingly, the groups treated intraductally with both free curcumin and NanoCurc had a similar decrease in the expression of Ki67. The main mechanism behind the action of NanoCurc was via regulating cell proliferation, which was evident by the decrease in the mitosis marker phospho-histone H3 (Chun *et al.*, 2012).

In a recent study, Liu *et al.* studied the efficacy of curcumin loaded polymeric micelles (Cur-M) via passive targeting, as a drug for breast cancer using the highly metastatic 4T1 mouse mammary tumour cell line in BALB/c mice. Cur-M had an encapsulation efficiency of 99% and showed a sustained release rate. Both free curcumin and Cur-M demonstrated concentration-dependent cytotoxicity in 4T1 cell line, but Cur-M produced a statistically significant cytotoxicity at a curcumin concentration of 20 µg/mL. The Cur-M-treated mice (30 mg/kg) when compared to control, showed a 76% reduction in tumour burden, a significantly higher (45%) median survival, and a 79% reduction in tumour nodules in the lungs. Moreover, tumour tissues from Cur-M-treated mice had more apoptotic cells (16%) compared to control (2%), a 73% smaller CD31 mean microvessel density (MVD), and decrease in proliferation of cells evident by a weak Ki-67 immunoreactivity (25% for Cur-M, 68% for control) (Liu *et al.*, 2013).

1.7 Curcumin Analogues

An alternative approach to overcome the problems associated with curcumin is the synthesis of curcumin analogues by modifying the chemical structure of curcumin. Chemically, curcumin is a bis-α, β-unsaturated β-diketone which acts as a linker for two *o*-methoxy phenols attached to two terminal positions. The molecule exhibits keto-enol tautomerism at physiological pH, but the bis-keto form predominates in acidic and aqueous neutral solutions (Padhye *et al.*, 2010, Chakraborti *et al.*, 2013). It has been reported that the instability of curcumin is due to the enolic – OH moiety and the presence of the β-diketone moiety is not a definite prerequisite for curcumin's anti-cancer activities as curcumin analogues without them show anti-proliferative activity (Chakraborti *et al.*, 2013). By modifying the phenolic ring as well as the β-diketone moiety, a wide range of

curcumin analogues have been synthesised that are more potent than curcumin (Mosley *et al.*, 2007). Analogues having the cyclohexanone ring are referred to as the first-generation analogues. The cyclohexanone containing derivative 2, 6-bis ((3- methoxy-4-hydroxyphenyl) methylene)-cyclohexanone (BMHPC) had an IC_{50} value of 5.0 µM and elicited cytotoxicity, anti-angiogenic properties against MDA-MB-231 and murine endothelial cells (Adams *et al.*, 2004) (Figure 2).

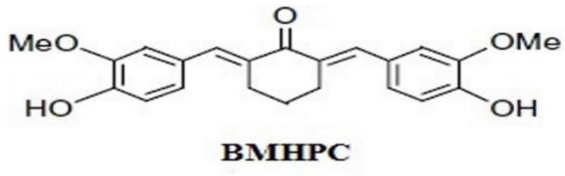

Figure 2: Chemical structure of BMHPC (Adams *et al.*, 2004).

Among all the analogues, the fluorinated compound EF24 (3, 5-Bis-(2-fluorobenzylidene)-piperidin-4-one, acetic acid salt) demonstrated the most potent cytotoxicity in MDA-MB-231 cells with an IC_{50} value of 0.8 µM ±0.4. EF24 at 100 mg/kg also elicited tumour regression by 45% compared to control in a xenograft model of MDA-MB-231 cells, at a dose lower than the maximum tolerated dose (MTD) of 200 mg/kg i.v. without any toxicity (Adams *et al.*, 2004) (Figure 3). EF24 at 10 µM inhibited cell proliferation and induced growth arrest in G2/M phase of the cell cycle in ER (-) breast cancer cells. EF24 caused apoptosis by caspase-3 activation, phosphatidylserine externalisation and by depolarisation of the mitochondrial membrane potential (Adams *et al.*, 2005). Studies focussing on the mechanism of action of EF24 in MDA-MB-231 cells showed that the analogue elicited its anti-proliferative activity by down-regulating the expression of the pro-angiogenic transcription factor hypoxia inducible transcription factor (HIF-1) post-transcriptionally in a von hippel landau- (VHL) dependent, but proteasome- independent mechanism (Thomas *et al.*, 2008). EF24 also demonstrated anti-angiogenic action when conjugated with coagulation factor VIIa (fVIIa) to target tissue factor (TF), which is overexpressed in tumour vascular endothelial cells. The conjugate induced apoptosis in MDA-MB-231 and HUVEC cells. Intravenous injections of the conjugate containing 50 µM of EF24 significantly reduced tumour burden (approximately 45%) in a MDA-MB-231 xenograft model (Shoji *et al.*, 2008).

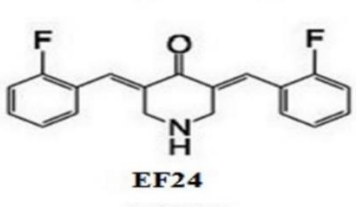

Figure 3: Chemical structure of EF24 (Thomas *et al.*, 2008).

By exchanging the β-diketone moiety for an αβ-unsaturated ketone, Lin *et al.* studied the effect of curcumin analogues FLLL11 and FLLL12 in different ER (+) and ER (-) breast cancer cells (Figure 4). Compared to curcumin, FLLL11 and FLLL12 had much lower IC_{50} values: 0.3-5.7 µM and 0.3-3.8 µM, respectively. At a concentration of 10 µM, the

analogues down-regulated the expression of Akt, STAT3, and Her2. They were also more effective than curcumin in inhibiting cell migration, colony formation, and inducing apoptosis. Moreover, these analogues together with doxorubicin elicited a more pronounced inhibition on cell viability, compared to doxorubicin or the analogues alone. MDA-MB-231 cells were treated with doxorubicin at different concentrations and cell viability was determined 72 h after treatment. The viable cells were approximately 55% for 200 nM and 37% for 400 nM. Similarly, the viable cells were approximately 37% with 5 μM of FLLL11. When the drugs were combined, synergism was observed with all the three different combinations of doxorubicin and FLLL11. The most potent effect was observed for the concentration 400 nM: 5 μM (doxorubicin: FLLL11), with approximately 18% of the cells being viable. A similar study was performed with doxorubicin and FLLL12. Approximately, 38% and 35% of MDA-MB-231 cells were viable after treatment with 400 nM and 5 μM of doxorubicin and FLLL12, respectively. Synergism was observed with all the three different combinations of doxorubicin and FLLL12. Specifically, treatment at concentrations 100 nM: 5 μM and 400 nM : 5 μM resulted in approximately less than 10% viable cells 72 h after treatment (Lin *et al.*, 2009).

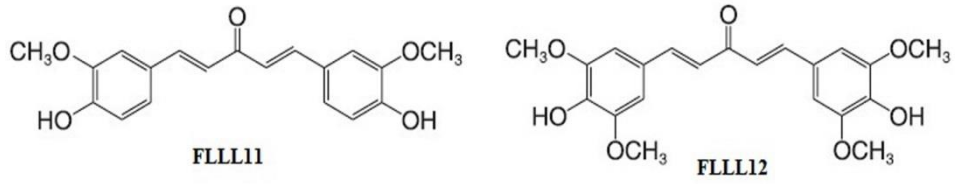

Figure 4: Chemical structure of FLLL11 and FLLL12 (Lin *et al.*, 2009).

In another study, more than 50 curcumin analogues were synthesised and screened by Ohori *et al.* Several curcumin analogues displayed enhanced efficacy and decreased the levels of oncoproteins at a much lower concentration than curcumin. These analogues were symmetrical 1, 5-diarylpentadienone with an alkoxy substitution at positions 3 and 5 of the aromatic rings. During their study, the authors found that addition of a methyl group to the *p*-hydroxy group relative to the β- unsaturated ketone moiety caused enhanced cytotoxicity and the presence of a 5-carbon tether was more efficacious than a 7-carbon tether (Ohori *et al.*, 2006). GO-Y030, one of the potent compounds from the aforementioned screening had an IC_{50} value of 1.2 μM compared to 19.3 μM for curcumin in MDA-MB-231 cells. At concentrations as low as 2.5 μM, GO-Y030 induced apoptosis by PARP cleavage and inhibited STAT3 phosphorylation at 5 μM. Also, 1 μM treatment of MDA-MB-231 cells with the analogue decreased colony formation by 95%, compared to control (Hutzen *et al.*, 2009) (Figure 5).

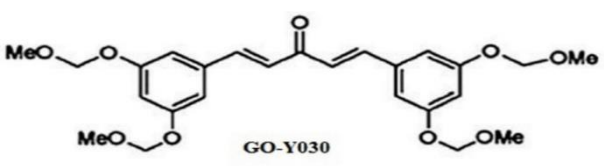

Figure 5: Chemical structure of GO-Y030 (Hutzen *et al.*, 2009).

By replacing the diketone moieties of natural curcumin analogues demethoxycurcumin and bisdemethoxycurcumin with hydrazine derivatives, Shim *et al.* synthesised a novel synthetic curcumin analogue called hydrazinocurcumin (HC) (Shim *et al.*, 2002). HC had IC_{50} values of 3.37 and 2.56 µM in MDA-MB-231 and MCF-7 cells, respectively, and elicited a concentration-dependent inhibition of cell viability 72 h after treatment. HC inhibited colony formation by 95% compared to control at 5 µM and elicited cell cycle arrest at the G1 phase at 10 µM, in both the cell lines. Concentration-dependent anti-apoptotic action was also seen 48 h post treatment, with 10 µM treatment causing 14% and 26% cells to undergo apoptosis in MDA-MB-231 and MCF-7 cells, respectively. HC at 10 and 20 µM treatment for 24 h in both the cell lines decreased STAT3 phosphorylation and inhibited its downstream targets such as MMP-9, MMP-2, Mcl-1, cyclin D1, c-Myc, Bcl-xl, survivin, and VEGF. Moreover, HC was more potent than curcumin at reducing the migration and invasion in both the cell lines (Wang *et al.*, 2012) (Figure 6).

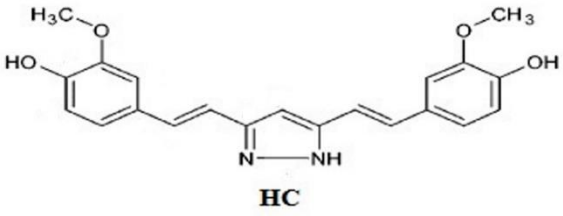

HC

Figure 6: Chemical structure of HC (Shim *et al.*, 2002).

By introducing benzimidazole groups into the feruloyl scaffold, 16 curcumin analogues were synthesised and tested for cytotoxicity, among which the compound 15H had an IC_{50} value of 1.9 µM against ER (+) breast cancer cell line MCF-7 (Woo *et al.*, 2012) (Figure 7).

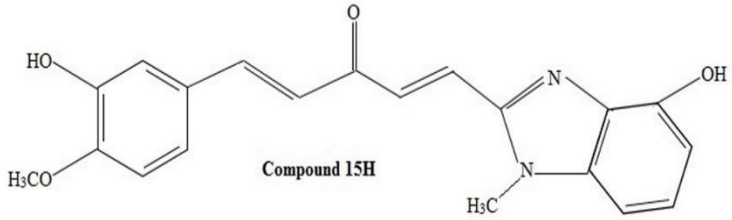

Compound 15H

Figure 7: Chemical structure of Compound 15H (Woo *et al.*, 2012).

Fuchs *et al*. synthesised a series of heptadiendione analogues (compounds 1-13) and pentadienone analogues (compounds 13-24). Among all the analogues, compound 23 was the most potent with an IC_{50} value of 0.4 and 0.6 µM in MCF-7 and MDA-MB-231 cells, respectively (Fuchs *et al.*, 2009) (Figure 8).

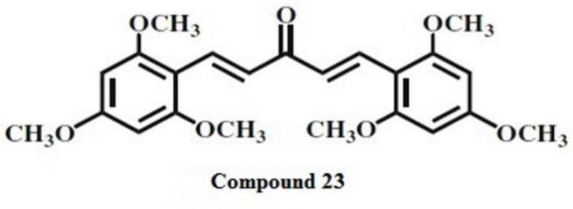

Figure 8: Chemical structure of compound 23 (Fuchs *et al.*, 2009).

Mono ketone analogues with a piperidone ring also displayed potent cytotoxicity when compared to curcumin. Specifically, compound 18 with N-ethylpiperidone ring was the most potent with IC_{50} values ranging from 2.6-5.5 µM in different breast cancer cells (Youssef and El-Sherbeny, 2005) (Figure 9).

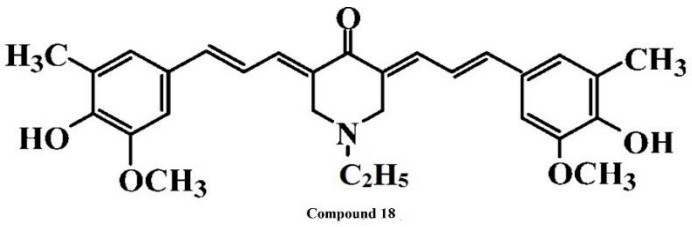

Figure 9: Chemical structure of compound 18 (Youssef and El-Sherbeny, 2005).

Another novel curcumin analogue, 5-bis (4-hydroxy-3-methoxybenzylidene)-N-methyl-4-piperidone (PAC) was synthesised by removal of methylene, carbonyl groups and introducing an N-methyl-4-piperidone into the curcumin structure (Figure 10). It was 5 times more potent than curcumin in apoptotic induction and was 10 times more potent in ER (-) breast cancer cells than ER (+) cancer cells. Treatment of MDA-MB-231 cells with 10 µM of PAC caused cell-cycle arrest at G2/M phase. PAC mediated its effect by decreasing the expression of NFκB, survivin, cyclin D1, Bcl-2 and up-regulating the expression of p21 *in vitro* and *in vivo*. In xenograft models of MDA-MB-231, PAC at 100 mg/kg/day significantly reduced tumour volume and triggered apoptosis. Moreover, PAC significantly increased bioavailability (5-fold) an hour after injection, and solubility (27-fold), when compared to curcumin (Al-Hujaily *et al.*, 2011).

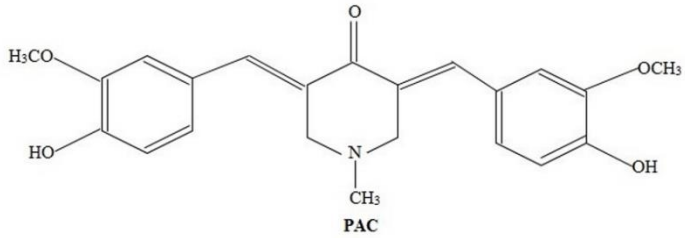

Figure 10: Chemical structure of PAC (Al-Hujaily *et al.*, 2011).

Studies have also been conducted to test the efficacy of curcumin analogues on 7, 12-dimethylbenz[a]anthracene (DMBA)-induced mammary carcinogenesis in mice. Dibenzoylmethane (DBM) is a chemical analogue of curcumin and lacks the phenolic hydroxyl groups on the aromatic rings (Figure 11). Female Sencar mice were either dosed with DMBA (1 mg per mouse, once weekly for 5 weeks) and AIN-76A diet (control) or 1% DBM in AIN-76A diet, beginning two weeks prior to the first dose of DMBA and continuing until they were sacrificed. The mice were sacrificed at 20 weeks after the last dose of DMBA treatment. Mice dosed with 1% DBM in their diet showed decreased mammary tumour multiplicity, tumour incidence, and increased latency time. Three weeks after the last dose of DMBA treatment, the first tumours appeared in the control group, whereas in the mice fed with 1% dietary DBM, the first tumours appeared 18 weeks after the cessation of DMBA treatment. Tumour incidence was also reduced by 97-100%. Dietary DBM treatment also resulted in inhibition of the proliferation rate of the mammary gland epithelial cells by 53%, and formation of DMBA-DNA adducts in mammary glands by 72%. Mechanistic studies showed that dietary DBM lowered serum oestradiol levels, increased the levels of hepatic cytochrome P450 enzymes, and increased hepatic hydroxylation and glucuronidation of oestradiol. *In vitro* studies showed that DBM competed with oestradiol for oestrogen receptor sites and elicited concentration-dependent inhibition of DMBA hydroxylation (Lin *et al.*, 2001, Lin *et al.*, 2001).

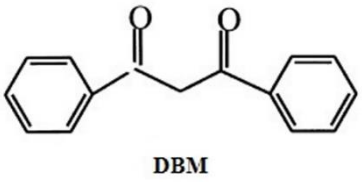

DBM

Figure 11: Chemical structure of DBM (Lin *et al.*, 2001).

Synthesis of second-generation curcumin analogues involves the modification of the central structure of the curcumin moiety by the introduction of heterocyclic rings. 18 curcumin analogues were synthesised, some of which elicited potent cytotoxicity in ER (-) breast cancer cell lines, MDA-MB-231 and SKBr3, compared to curcumin (Yadav *et al.*, 2010). Mechanistic studies of two analogues, 2, 6-bis (pyridin-3-ylmethylene)-cyclohexanone (RL90) and 2, 6-bis (pyridin-4-ylmethylene)-cyclohexanone (RL91) (Figure 12) showed their ability to modulate the expression of cell signalling proteins such as NFκB, Akt, EGFR, β-catenin, and Her2. Treatment with these analogues also resulted in the activation of stress kinases by phosphorylation of JNK1/2 and p38 MAPK. In MDA-MB-231 cells, 3 μM of RL90 or 2.5 μM of RL91 caused cell cycle arrest in G2/M phase. Compared to control, the number of apoptotic cells increased by 164% and 406% with RL90 and RL91, respectively (Somers-Edgar *et al.*, 2011).

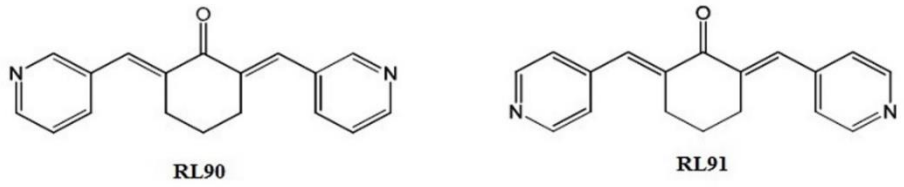

Figure 12: Chemical structure of RL90 and RL91 (Leung *et al.*, 2012).

More potent analogues were obtained by modification of the curcumin scaffold to include N-methylpiperidone, tropinone or cyclopentanone core groups. In MDA-MB-231 cells, 3,5-bis (pyridine-4-yl)-1-methylpiperidin-4-one (RL66) and 3,5-bis (3,4,5-trimethoxybenzylidene)-1 methylpiperidin-4-one (RL71) (Figure 13) had IC_{50} values of 0.8 and 0.3 µM, respectively (Yadav *et al.*, 2010). In SKBr3 cells, RL71 at 1 µM induced cell cycle arrest in G2/M phase, time-dependent anti-apoptotic effect with 35% cells undergoing apoptosis after 48 h, and increased the expression of cleaved caspase-3 and p27. RL71 also down- regulated the expression of Her2 phosphorylation with complete inhibition after 12h. In MDA-MB-231 and MDA-MB-468 cells, RL71 (1 µM) significantly down-regulated the expression of Akt phosphorylation and transiently increased the stress kinases JNK1/2 and p38 MAPK. RL71 also elicited anti-angiogenic properties by inhibiting HUVEC cell migration (46% compared to control) and their ability to form endothelial tubes. RL71 at 8.5 mg/kg was also orally bioavailable and produced a peak plasma concentration 5 min after oral dosing (Yadav *et al.*, 2012). RL66 also had a similar mechanism of action in ER (-) breast cancer cell lines. Treatment of SKBr3 cells with 2 µM of RL66 resulted in cell cycle arrest, apoptosis, decrease in Her2 phosphorylation, and increase in the expression of p27, caspase-3 48 h post treatment. RL66 at 2 µM down-regulated the expression of Akt phosphorylation and transiently increased the stress kinases JNK1/2 and p38 MAPK. RL66 inhibited HUVEC cell migration by 46% and endothelial tube formation. Importantly, RL66 at 8.5 mg/kg by oral dosing daily, for 10 weeks, suppressed tumour growth in a MDA-MB-468 xenograft model by 48% and decreased the MVD in the tumours by 57%, when compared to control. Thus, RL66 demonstrated potent anti-cancer activity *in vitro* and *in vivo* (Yadav *et al.*, 2012).

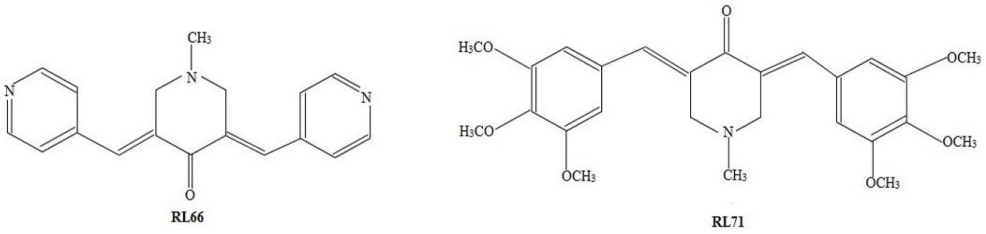

Figure 13: Chemical structure of RL66 and RL71 (Yadav *et al.*, 2012, Yadav *et al.*, 2012).

A series of mono-carbonyl curcumin analogues have been synthesised by deleting the β-ketone moiety, considered responsible for the limitations of curcumin. The synthesis of these compounds involved different 5-carbon linkers such as cyclopentanone, acetone and cyclohexanone. The analogues exhibited an increased stability and pharmacokinetic profile. Oral dosing of male Sprague-Dawley rats with 500 mg/kg of compound B02 and

B33 (Figure 14) resulted in an increase in the plasma concentration to 0.82 µg/ml and 4.1 µg/ml, respectively, whereas curcumin had a plasma concentration of 0.091 µg/ml. There was also a decrease in the plasma clearance of the compound B02 (125.4 L/kg/h) and B33 (38.98 L/kg/h), compared to curcumin (835.2 L/kg/h). The half-life of B02 was twice that of curcumin. Furthermore, there was an increase in the cytotoxicity of these analogues towards tumour cell lines by the replacement of benzene ring with a hetero aromatic ring (Liang *et al.*, 2009).

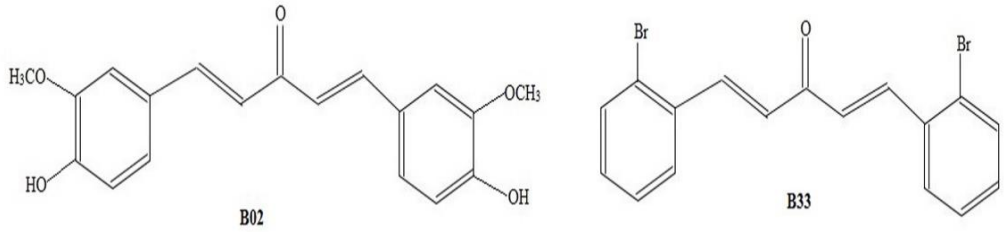

Figure 14: Chemical structure of B02 and B33 (Liang *et al.*, 2009).

1.8 Nanotechnology to Improve Curcumin Analogue's Pharmacokinetics

Though majority of curcumin analogues synthesised are more potent and stable than the parent compound in breast cancer cell lines, the same problem with curcumin was seen when the analogues were tested in xenograft models. For example, the most potent curcumin analogue, RL71, showed limited *in vivo* activity due to limited solubility, bio-distribution and stability (Taurin *et al.*, 2013). Other laboratories are also now focusing on nanoparticle formulation of curcumin analogues to further improve the efficacy of the drug and achieve tumour specific targeting (Agashe *et al.*, 2011, Zhang *et al.*, 2013).

To improve the efficacy of RL71, SMA micelles were used as a drug carrier because of their amphiphilic nature and ability to improve the pharmacokinetics of the drug (Figure 15). Different loadings of SMA-RL71 (5, 10, and 15%) were prepared and their physiochemical characteristics were assessed. The cytotoxicity of SMA-RL71 was also compared with free RL71 in different TNBC cell lines. The micelles had a near neutral zeta potential and 15% loading had a slower release rate, and higher cellular uptake. 15% SMA-RL71 was more stable than free RL71 and elicited a higher cytotoxicity with an IC_{50} value of 0.54 µM in MDA-MB-231 cells. The 15% SMA-RL71 was also cytotoxic in a tumour spheroid model. Overall, 15% SMA-RL71 showed characteristics favourable for preclinical studies in xenograft models (Taurin *et al.*, 2013).

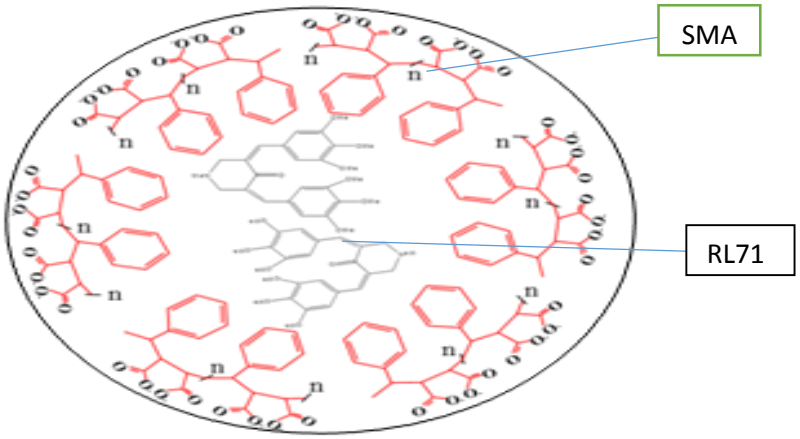

Figure 15: Structure of SMA-RL71. The styrene group of SMA forms the hydrophobic core of the micelle. The ionised COOH group of maleyl residues of SMA forms the hydrophilic group and gives the property of aqueous solubility to the drug. Diagram adapted from (Iyer *et al.*, 2007).

Hydrazinocurcumin, a curcumin analogue described in earlier sections, was also encapsulated in a nanoparticle (HC-NP) and tested for its effect on the tumour microenvironment in breast cancer cell lines and animal models. The local tumour microenvironment can recruit and program tumour associated macrophages (TAMs) to transform into a tumour initiating phenotype called M2 having the following expressions: IL-10 (high), IL-12 (low), and TGF-β (high). STAT3 signalling plays a crucial role in malignancy through crosstalk between tumour cells and TAMs. Co-culture of 4T1 mouse breast cancer cells with RAW264.7 cells resulted in a transformation from M1 to M2 phenotype. The RAW264.7 cells referred in this step as 'educated' (E-RAW264.7) were re-educated (RE-E- RAW264.7) when treated with 18 μM of HC-NP, resulting in the transformation of M2 phenotype to M1 phenotype macrophages with the following characteristics: IL-10 (low), IL-12 (high), and TGF-β (low). Cell migration and invasion were affected by a decrease in the expression of pSTAT3, MMP-9, MMP-2, and VEGF. The treatment also resulted in a decrease in the number of cells in the S-phase (38%) compared to control (54%). Treatment of BALB/c female mice with 1 mM of Legumain-targeting-HC-NPs (Leg-HC-NPs) 10 days after tumour induction, at 3 day intervals within 15 days resulted in a significant decrease in tumour weight by approximately 71% and an increase in survival by more than 2 months. Immunohistochemical analysis showed that the percentage of Ki67-positive cells in the Leg-HC-NPs group was approximately 18%, compared to 68% for control, while the percentage of STAT3-positive cells was approximately 15%, compared to 50% for control. Furthermore, there was a 70% decrease in CD31-positive MVD in the Leg-HC-NPs group compared to control. Moreover, Leg-HCNPs-treated mice had a 3-fold decrease in pulmonary metastasis when compared to control (Zhang *et al.*, 2013).

1.9 Aims

Since 15% SMA-RL71 showed promising anti-cancer activity *in vitro*, the aim of the present study was to

i) evaluate the efficacy of 15% SMA-RL71 in eliciting tumour suppression in animal models of breast cancer.

ii) evaluate the toxicity profile of SMA-RL71 by assessing the physiological parameters of animal health.

iii) optimise HPLC for detection of RL71.

Chapter Two: Methods

2.1 Chemicals

All the RL compounds used in the study were synthesised at the Department of Chemistry, University of Otago as previously described (Yadav *et al.*, 2010). HPLC grade acetonitrile and methanol were purchased from Merck (USA). Reagent grade glacial acetic acid was purchased from Scharlab S.L. (Spain). Curcumin was purchased from Cayman Chemical (Michigan, USA). Cumene terminated poly(styrene-co-maleic anhydride) with an average Mn ~ 1700, N-(3-dimethylaminopropyl)-N-ethyl- carbodiimide hydrochloride (EDAC) were obtained from Sigma- Aldrich Ltd. (St.Louis, MO). Milli-Q water with a resistance value of 18.3 MΩ/cm was obtained from a Milli-Q Synthesis Water System (Millipore, MA). MDA-MB-231 breast cancer cells were purchased from American Type Culture Collection (Manassas, VA). Matrigel was purchased from BD Biosciences (San Diego, CA). EDTA and sodium bicarbonate were purchased from BDH Laboratory Supplies (Poole, U.K.). OCT compound was purchased from CellPath (Newton, U.K.). N-hexane was purchased from Fluka (Germany). Bovine serum albumin (BSA) and trypsin were purchased from Gibco (Auckland, New Zealand). Foetal bovine serum (FBS) was purchased from Invitrogen (Auckland, New Zealand). Sodium chloride (NaCl) was purchased from Merck (Darmestadt, Germany). Dulbecco's Modified Eagle's media (DMEM), hydrochloric acid (HCl, 37%), MEM media, methanol (99.8%), Tris[hydroxymethyl]aminomethane hydrochloride (Tris-HCl), and nutrient mixture Ham's F-12 media were purchased from Sigma Aldrich (St. Louis, MO).

2.2. Cell Maintenance

MDA-MB-231 breast cancer cells were maintained in minimum essential medium (MEM) supplemented with 5% foetal bovine serum, 2 mM L-glutamine, 100 U/mL penicillin, 100 µg/mL streptomycin and 2.2 g/L of sodium bicarbonate. Cells were cultured in 75 cm^2 flasks and were incubated at 37° C, 5% CO_2, 95% humidified air. The solutions were warmed to 37°C and the flasks containing MDA-MB-231 cells were passaged upon reaching 90% confluency. The cells were then washed with phosphate buffered saline solution (PBS) and incubated with trypsin solution (2.69 mM EDTA, 1g/L trypsin, 0.14 M NaCl, 76.78 mM tris HCl; pH 8) for 2 min to detach the cells from the flask. This was followed by the addition of complete growth media and transfer of the contents into a 50 mL conical tube. The supernatant was discarded after the cells were centrifuged at 1200 rpm for 3 min. The pellet was resuspended in fresh media and 15 µL of the suspension was used to count the cells on a haemocytometer.

2.3. SMA-RL71 Micelle Preparation (15% loading)

15% loading of SMA-RL71 was prepared as described below. RL71 dissolved in 1 mL of DMSO and EDAC dissolved in 1 mL of Milli-Q water were added to the hydrolysed SMA solution (pH 5). The pH was adjusted again to 5 after adding the drug and EDAC by adding 1 M HCl (drop wise). The pH was then increased to 11 by adding 1 M NaOH and left for few minutes for the pH to decrease slowly. The pH was then decreased to 3 and the solution centrifuged at 3000 rpm for 5 min (Eppendorf 5810R centrifuge). The pellet was

dissolved in Milli-Q water and the pH taken to 7.4 by adding 0.1 N NaOH. The micellar solution was subjected to four rounds of ultrafiltration using Pellicon XL filter 10 kDa (Merck Millipore, Auckland, New Zealand) and then lyophilised to obtain the powder form of SMA-RL71.

2.4. Animal Housing and Care

Female SCID mice (2-2.5 months) were purchased from the Animal Resources Centre (Murdoch, Western Australia). All animal experiments were carried out with prior approval from the animal ethics committee (AEC # 41/11). The animals were housed under sterile conditions under 12 hour dark/light cycle at 21-24°, with access to food and water *ad libitum*. They were allowed to acclimate for three days before beginning the experiment.

2.5. Tumour Implantation and Dosing Regimen

On the day of tumour inoculation, a cell suspension of MDA-MB-231 cells (1 x 10^6 cells/mL) in MEM growth media and Matrigel (1:1 ratio) was prepared by Dr.S.Taurin and kept on ice. 50 µL of the suspension was then subcutaneously injected into both the flanks of the mice by Dr.S.Taurin. They were left for two weeks for palpable tumours (100 mm^3) to form. Mice were then randomly assigned to different treatment groups and dosed via tail vein injections by Dr.K.Greish.

For the dose response study, mice were assigned into groups: control, SMA-RL71 5 mg/kg, SMA-RL71 10 mg/kg, SMA-RL71 15 mg/kg, and RL71 10 mg/kg. The control group received tail vein injections of sodium hydrogen carbonate pH 8, 0.1 M. They were dosed on days 1 and 8. The duration of the study was 29 days and there were 5 mice in each treatment group. Tumour measurement and weight of the animals were checked thrice a week. Tumour volume was measured thrice a week using a digital calliper and calculated using the formula length/2*$(width)^2$.

For the time course study, 10 mg/kg was chosen as the dose and dosed at different time points to test the tumour suppressive effect of the drug. Mice were grouped into control, SMA-RL71 10 mg/kg (twice weekly, every 3-4 days for 2 weeks), SMA-RL71 10 mg/kg (twice weekly, every 3-4 days for 3 weeks), RL71 10 mg/kg (twice weekly, every 3-4 days for 2 weeks), and RL71 10 mg/kg (twice weekly, every 3-4 days for 3 weeks). The control group mice received tail vein injections of PBS. All mice were dosed twice weekly. The duration of the study was 31 days. Tumour measurement and weight of the animals were checked twice a week. Tumour volume was measured twice a week using a digital calliper and calculated using the formula length/2*$(width)^2$.

2.6. Tissue and Blood Collection

At necropsy, the animals were euthanized by CO_2 inhalation. Blood was drawn from the inferior vena cava using a heparinised syringe and centrifuged at 3,000 rpm for 10 min (Eppendorf 5810R centrifuge) to separate plasma, which was transferred into Eppendorf tubes and stored at -80°C. Tumours, liver, kidneys, spleen, and uterus were harvested, weighed, frozen in liquid nitrogen or OCT compound (in N-hexane) and stored at -80°C for later use. Liver, spleen, kidney, and tumours which were to be used for immunohistochemistry were fixed in OCT compound in tinfoil boats. They were then first

placed in a beaker containing N-hexane and after they were frozen, they were stored in liquid nitrogen and then at -20°C for later use.

2.7. Method Development for HPLC

2.7.1. HPLC Conditions

Samples were analysed using a Shimadzu Prominence LC-20A Series HPLC system consisting of a binary pump (LC-20AD), UV/VIS PDA detector (SPD-M20A), online degasser (DGU-20A3R), an auto sampler (SIL-20A), and a column oven (CTO-20A) maintained at 30°C with a C18 column (Phenomenex Gemini- NX) 5µ (150 x 4.6 mm) fitted with a C18 guard column (4 x 3.0 mm). The PDA had a slitwidth of 1.2 nm, bandwith of 4 nm and was maintained at 40°C. The HPLC machine was run in an isocratic mode with 65% acetonitrile and 10 mM pH 5 acetate buffer as mobile phase. Absorbance of RL71 and curcumin were analysed at 361 nm and 425 nm, respectively. The mobile phase was delivered at a flow rate of 1 mL/min and the injection volume was 10 µL. The runtime was 10 minutes. The acetate buffer was filtered through a 0.45 µm nylon filter (Phenomenex, North Shore City, New Zealand). A vial of 100% methanol was run after the highest concentration of the compound to assess carryover.

2.7.2. Stock, Working and Internal Standard Solutions

The stock (1 mg/mL) and working standards of RL71 were prepared by dissolving in methanol. Serial dilutions were then performed to obtain desired concentrations for the calibration curve (0.1 µg/mL, 0.5 µg/mL, 2 µg/mL, 10 µg/mL and 50 µg/mL). All the working standards were spiked with 20 µL of 100 µg/mL curcumin. The internal standard was prepared by dissolving curcumin powder in methanol to obtain a stock solution of 200 µg/mL and diluted to obtain a concentration of 100 µg/mL, from which 20 µL (final concentration of 2 µg/ml curcumin in the vials) was added to all the calibration standard solutions of RL71.

2.7.3. Limit of Detection and Limit of Quantitation

The signal-to-noise-ratio (SNR) is a frequntly used parameter to determine the detector performance and the lower limit of detection (LOD) of an analyte (Miller, 2009). LOD is the lowest concentration of an analyte that cannot be quantified, but can be detected from background noise, with an SNR of at least 3 (Miller, 2009, Uney *et al.*, 2011, Shah *et al.*, 2013). Limit of Quantitation (LOQ) is the lowest concentration of an analyte that can be quantified with accuracy and precision, with an SNR of at least 10 (Miller, 2009, Uney *et al.*, 2011, Shah *et al.*, 2013). From the chromatograms obtained, LOD and LOQ were calculated using SNR. The signal and noise were calculated at the retention time of RL71 (4.5 min) using the chromatograms obtained for a methanol blank and RL71, respectively. Different concentrations of RL71 such as 10, 20, 40, 60, and 80 ng/mL, spiked with 20 µL of 100 µg/mL curcumin, were run to determine the LOD.

2.7.4. Sample Preparation for Plasma Extraction

Plasma samples for HPLC analysis were prepared by methanol extraction, which is as follows: To 180 µL of plasma, 20 µL of 10 µg/mL RL71 and SMA-RL71 dissolved in methanol were added. The samples were then mixed by inverting for 1 min and allowed to stand for 10 min. Then, 600 µL of methanol was added to the samples and sonicated for 10 min. To assess extraction efficiency, samples to allowed to stand for 1 h, 2 h, 3 h, and 24 h. After the respective time points, the samples were centrifuged at 13,000 rpm for 15 min. The clear supernatant (500 µL) was transferred into amber coloured HPLC vials and spiked with 10 µL of 100 µg/mL curcumin. The pellet was lyophilised and stored at -80°C for further extraction. Furthermore, 20 µL of 10 µg/mL free and micellar drug were made up to 500 µL using methanol and spiked with 10 µL of 100 µg/mL curcumin, to compare the peaks for the compound just dissolved in methanol versus the one that has been subjected to methanol extraction. To determine the recovery of RL71 in extracted plasma, different concentrations of RL71 (40, 60, 80, and 200 ng/mL) were added to the plasma, methanol extracted and spiked with 10 µL of 100 µg/mL curcumin.

2.7.5. Surrogates for Plasma Extraction

In order to compensate for the loss of RL71 during methanol extraction, a series of RL compounds, raloxifene, and 4-methoxybenzophenone (at 50 µg/mL) were screened for their suitability as a surrogate. Only compounds that have did not have similar retention times as that of curcumin (3.47 min) and RL71 (4.5 min) were chosen and methanol extracted in plasma along with the addition of 20 µL of 10 µg/mL RL71. The supernatants from plasma extraction (500 µL) were then spiked with 10 µL of 100 µg/mL curcumin and analysed.

2.8. Statistical Analysis

Statistical analyses were performed using GraphPad Prism software (Graph-Pad Software, Inc., San Diego, CA, USA).To determine the statistical significance between tumour volume of the treated groups, two-way (repeated measurements) analysis of variance (ANOVA) followed by Bonferroni post-tests were carried out. To determine the statistical significance between the organ weights of the treated groups, one-way analysis of variance (ANOVA) followed by Dunnett's post-tests were carried out. Values that differed significantly in variance were log transformed and then subjected to post-tests. The minimum requirement for a statistically significant value was $P<0.05$.

Chapter Three: Results

3.1. Drug Efficacy

3.1.1. Dose Response

To determine if SMA-RL71 was effective in suppressing tumour growth in xenograft models, a dose response study was performed with different doses of SMA-RL71. By measuring the tumour volume and determining the organ weight on the day of sacrifice, the effect of drug was determined. On day 29, tumour volume was 306.7 ± 40.7, 364.2 ± 61.0, 340.1 ± 77.2, 367.3 ± 44.1 and 617.0 ± 113.8 for the control, SMA-RL71 15 mg/kg, SMA-RL71 10 mg/kg, SMA-RL71 5 mg/kg and RL71 10 mg/kg, respectively. No statistically significant reduction in tumour volume was observed (Figure 16). On day 29, the mice were sacrificed. There was no signficant reduction in the tumour weight. However, a significant increase ($p<0.0001$) in tumour weight of the mice dosed with the free drug was observed (Table 2). All mice gained a similar amount of body weight at the end of the study (Table 3). There was a statistically significant ($p<0.05$) increase in the liver weight of the mice dosed with SMA-RL71 10 mg/kg. The spleen weight was also significantly elevated ($p<0.05$) for the SMA-RL71 10 mg/kg (96%) and RL71 10 mg/kg-treated mice (70%) (Table 4).

Between day 15 and 22, a decrease in tumour volume (not statistically significant) was observed between the control and SMA-RL71 10 mg/kg-treated mice (Figure 17). Tumour suppression might have been achieved if the mice were dosed repeatedly. Though a similar effect was observed with SMA-RL71 15 mg/kg, the dose could not be used as it caused necrosis of the tail. Hence, SMA-RL71 10 mg/kg was chosen to detemine if changing the frequency of drug administration could increase the efficay of the drug. It was hypothesised that dosing the mice with multiple injections at different time points would elicit tumour suppression.

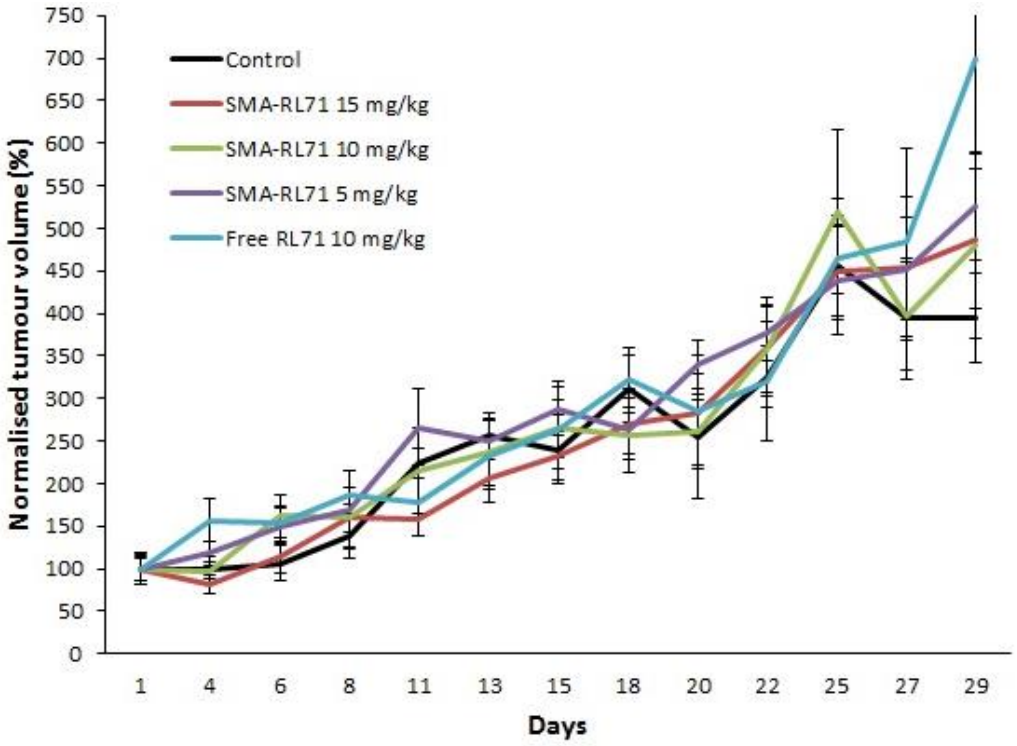

Figure 16: Effect of SMA-RL71 on tumour volume in xenograft model - dose response study. Female SCID mice were inoculated bilaterally in the flank with 1 x 10^6 MDA-MB-231 breast cancer cells and injected via the tail vein on day 1 and day 8 with either control (0.1 M, pH 8 $NaHCO_3$), SMA-RL71 15 mg/kg, SMA-RL71 10 mg/kg, SMA-RL71 5 mg/kg or RL71 10 mg/kg. The points represent the mean ± SEM. Two-way (repeated measurements) ANOVA followed by Bonferroni post-tests were used to check for statistical significance between the different groups. The minimum requirement for a statistically significant value was $P<0.05$. No statistical significance was observed between the treatment groups.

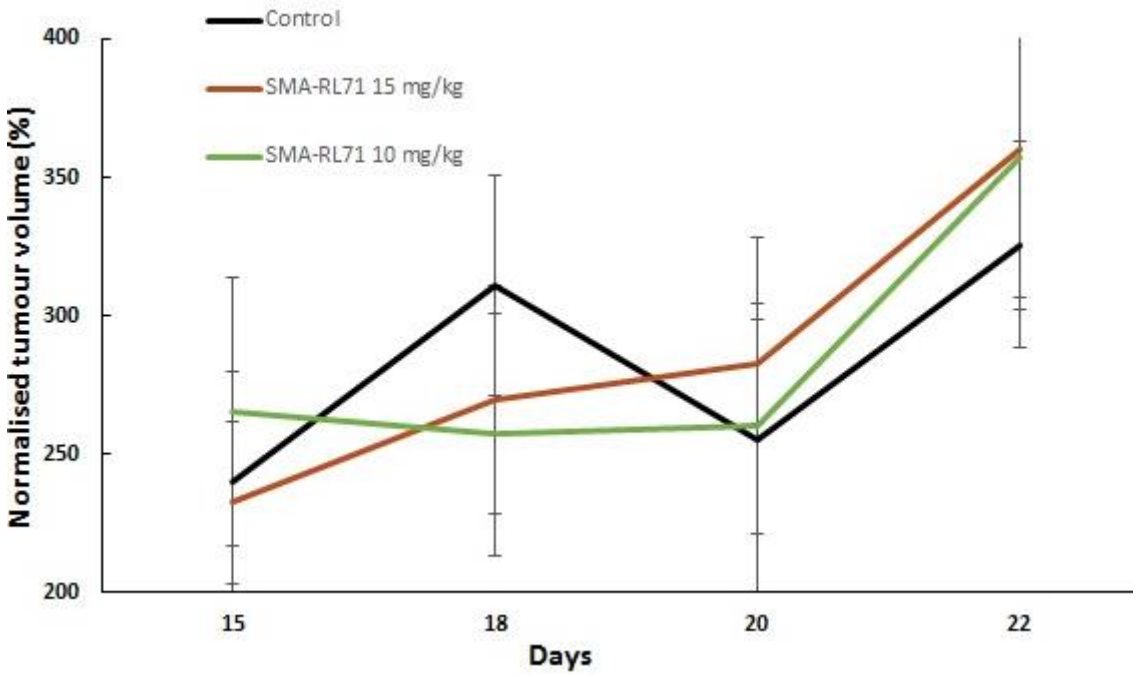

Figure 17: Effect of SMA-RL71 on tumour volume in xenograft model from day 15 to 22. Blown-up graph of mice dosed with control, SMA-RL71 (15 mg/kg) and SMA-RL71 (10 mg/kg) between day 15 to 22 to demonstrate that SMA-RL71 (10 mg/kg) elicited a decrease in tumour volume (not statistically significant), compared to control.

Table 2: Mean tumour weight (g) for each treatment group on day 29.

	Control	SMA- RL71 (15 mg/kg)	SMA-RL71 (10 mg/kg)	SMA-RL71 (5 mg/kg)	RL71 (10 mg/kg)
Tumour Weight (g)	0.25 ± 0.02	0.23 ± 0.01	0.27 ± 0.02	0.34 ± 0.03	**0.46 ± 0.04***

Data expressed as mean ± SEM
***** = $p<0.001$

Table 3: Mean weight gain (g) in mice at day 29

	Control	SMA-RL71 (15 mg/kg)	SMA-RL71 (10 mg/kg)	SMA-RL71 (5 mg/kg)	RL71 (10 mg/kg)
Mean weight gain (g)	2.4 ± 0.4	1.6 ± 0.4	2.4 ± 0.4	2.8 ± 0.49	2 ± 0

Data expressed as mean ± SEM
No comparisons were significantly different from the control.

Table 4: Mean organ weight (% of body weight) on day 29.

Treatment	Liver	Kidney	Spleen	Uterus
Control	4.38 ± 0.15	1.20 ± 0.02	0.3 ± 0.02	0.36 ± 0.06
SMA-RL71 (15 mg/kg)	4.71 ± 0.16	1.22 ± 0.07	0.43 ± 0.03	0.25 ± 0.02
SMA-RL71 (10 mg/kg)	**5.23 ± 0.09***	1.45 ± 0.15	**0.59 ± 0.09***	0.35 ± 0.03
SMA-RL71 (5 mg/kg)	4.07 ± 0.31	1.11 ± 0.07	0.49 ± 0.14	0.24 ± 0.07
RL71 (10 mg/kg)	4.61 ± 0.10	1.26 ± 0.03	**0.51 ± 0.05***	0.3 ± 0.04

Data expressed as mean ± SEM
*****=$p<0.05$

3.1.2 Time Course

To determine if tumour suppression could be achieved by increasing the frequency of the dose, multiple injections of SMA-RL71 (10 mg/kg) were used. Compared with the control group, the mice dosed with the micellar drug exhibited a significant decrease in tumour volume from day 18 ($P<0.001$) (Figure 18). Specifically, the reduction in tumour growth for the mice dosed every 3-4 days with the micellar drug for two weeks and three weeks were seen from day 24 and 18, respectively. On day 31, tumour volume in the control-treated mice was 241 ± 10.8 mm^3, whereas in the two weeks and three weeks SMA-RL71 10 mg/kg treated mice, the tumour volume was 130 ± 10.9 (46% decrease) and 177.2 ± 13.6 mm^3 (26% decrease), respectively when compared with the control group mice.

A statistically significant reduction ($p<0.0001$) in tumour weight was observed for the SMA-RL71 10 mg/kg two weeks treated-mice (Table 5). All mice gained a similar amount of weight at the end of the study (Table 6). The mean organ weight of the liver exhibited a statistically significant increase for the SMA-RL71 10 mg/kg (2 weeks)-treated ($p<0.05$)

and SMA-RL71 10 mg/kg (3 weeks)-treated mice ($p<0.0001$). A statistically significant increase ($p<0.05$) in kidney weight was observed for the mice dosed with SMA-RL71 10 mg/kg for 3 weeks and a statistically significant increase ($p<0.0001$) in spleen weight was also observed for both the SMA-RL71 10 mg/kg 2 weeks and 3 weeks-treated mice. The mice dosed with the micellar drug for three weeks exhibited signs of toxicity such as discolouration of liver and splenomegaly. The mice dosed with the micellar drug for two weeks also exhibited an increase in spleen weight. Specifically, compared to the control group, there was 96% and 217% increase in spleen weight for the SMA-RL71 10 mg/kg (2 weeks) and SMA-RL71 10 mg/kg (3 weeks) group. This was statistically significant ($p<0.0001$) (Table 7).

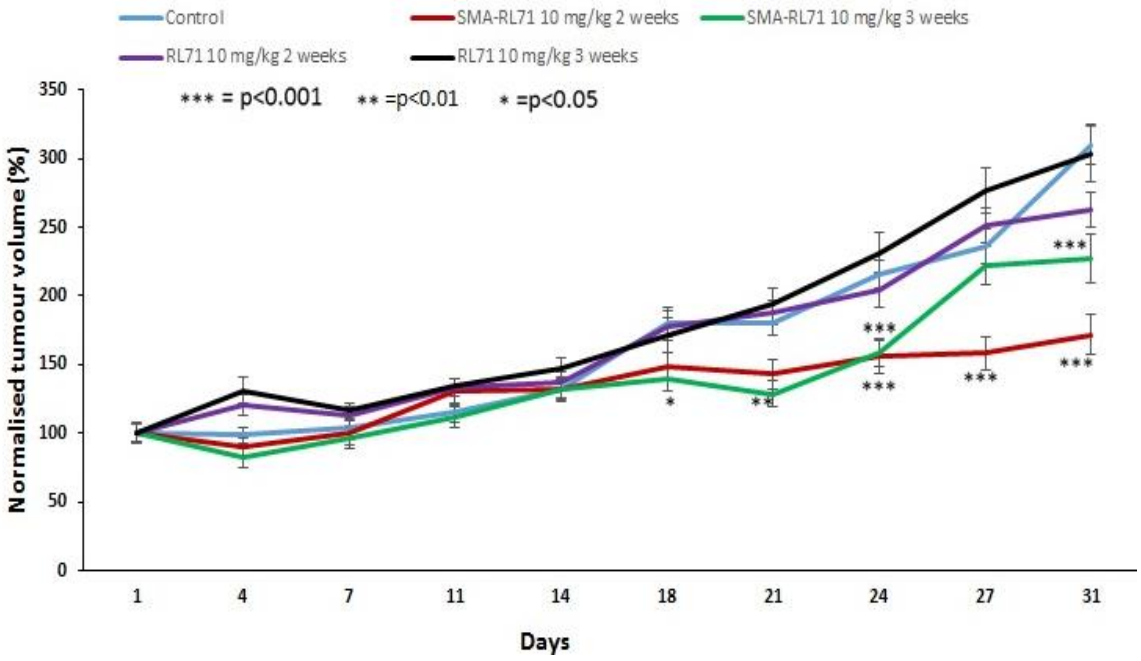

Figure 18: Effect of SMA-RL71 on tumour volume in xenograft model – time course. Female SCID mice were inoculated bilaterally in the flank with 1 x 10^6 MDA-MB-231 breast cancer cells and injected via the tail vein twice weekly with either control (PBS), SMA-RL71 10 mg/kg (2 weeks), SMA-RL71 10 mg/kg (3 weeks), RL71 10 mg/kg (2 weeks) or RL71 10 mg/kg (3 weeks). The points represent the mean ± SEM. Two-way (repeated measurements) ANOVA followed by Bonferroni post-tests were used to check for statistical significance between the different groups. The minimum requirement for a statistically significant value was $P<0.05$. Statistically significant difference in tumour volume was found for the SMA-RL71 (2 weeks) and SMA-RL71 (3 weeks) from day 24 and 18, respectively.

Table 5: Mean tumour weight (g) for each treatment group on day 31.

	Control	SMA-RL71 (10 mg/kg) (2 weeks)	SMA-RL71 (10 mg/kg) (3 weeks)	RL71 (10 mg/kg) (2 weeks)	RL71 (10 mg/kg) (3 weeks)
Tumour Weight (g)	0.21 ± 0.01	**0.12 ± 0.01***	0.18 ± 0.01	0.18 ± 0.007	0.19 ± 0.02

Data expressed as mean ± SEM
*= p<0.0001

Table 6: Mean weight gain (g) in mice at day 31

	Control	SMA-RL71 (10 mg/kg) (2 weeks)	SMA-RL71 (10 mg/kg) (3 weeks)	RL71 (10 mg/kg) (2 weeks)	RL71 (10 mg/kg) (3 weeks)
Mean weight gain (g)	2.49 ± 0.3	2.07 ± 0.24	1.7 ± 0.38	2.28 ± 0.28	2.38 ± 0.37

Data expressed as mean ± SEM
None were significantly different from the control.

Table 7: Mean organ weight (% of body weight) on day 31

Treatment	Liver	Kidney	Spleen	Uterus
Control	4.81 ± 0.13	1.21 ± 0.03	0.23 ± 0.01	0.35 ± 0.03
SMA-RL71 (10 mg/kg) (2 weeks)	**5.43 ± 0.11***	1.28 ± 0.01	**0.45 ± 0.02*****	0.34 ± 0.03
SMA-RL71 (10 mg/kg) (3 weeks)	**6.17 ±0.39*****	**1.44 ± 0.09***	**0.73 ± 0.09** ***	0.37 ± 0.02
RL71 (10 mg/kg) (2 weeks)	4.41 ± 0.13	1.26 ± 0.01	0.21 ± 0.01	0.27 ± 0.02
RL71 (10 mg/kg) (3 weeks)	4.45 ± 0.27	1.27 ± 0.02	0.25 ± 0.03	0.36 ± 0.04

Data expressed as mean ± SEM
***=p<0.0001, *=p<0.05

3.2 HPLC Optimisation

3.2.1 Method Development

In order to determine the amount of drug accumulation in plasma, tumours and tissues of mice dosed with SMA-RL71, HPLC with UV/VIS PDA detection with acetonitrile and 10 mM pH 5 acetate buffer as the mobile phase was used. Serial dilutions of RL71 from the stock solution (1 mg/mL) was performed with methanol to obtain the desired

concentrations (0.1, 0.5, 2, 10, and 50 µg/mL) for building a calibration curve (Table 8), using curcumin an internal standard. RL71 was detected at 361 nm and curcumin at 425 nm. A linear standrard curve was obtained with a r^2 value of 0.99996. The retention times of curcumin and RL71 were 3.4 and 4.49 min, respectively (Figure 19).

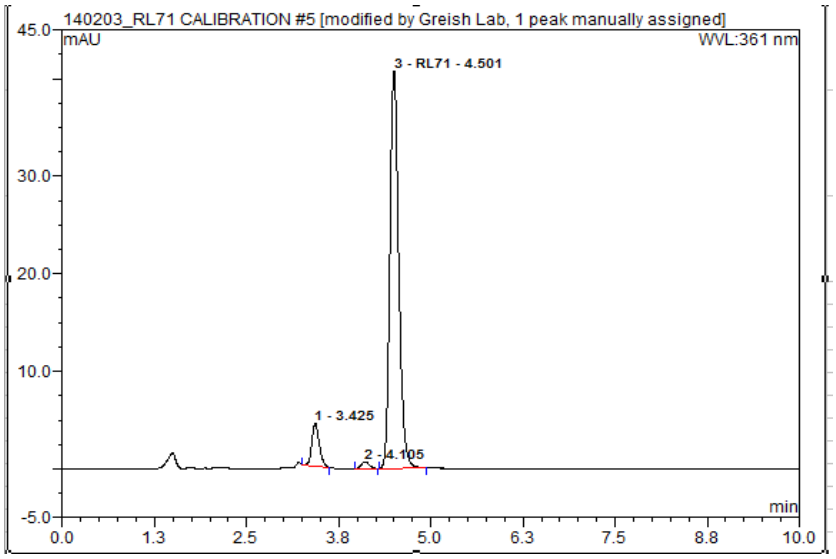

Figure 19: **Chromatogram of RL71**. 10 µg/mL of RL71 was spiked with 20 µL of 100 µg/mL curcumin.

Table 8: Summary of areas of different concentrations of RL71 using 65% acetonitrile and 10 mM pH 5 acetate buffer as mobile phase.

RL71 Concentration (µg/mL)	Area (mAU*min)
0.1	0.0453
0.5	0.2419
2	0.9550
10	5.6280
50	29.7430

3.2.2 Plasma Extraction of RL71

Plasma extraction was performed using the protocol mentioned earlier. 20 µL of 10 µg/mL of RL71 and 16.3% SMA-RL71 were added to the plasma and methanol extracted at various time points (t=1 h, 2 h, 3 h, and 24 h). The recovery for the free drug was 57.63%, 52.4%, 50.8%, and 48.78% at t=1 h, 2 h, 3 h, and 24 h, respectively. The recovery for the micellar drug was 59.45%, 54.4%, 55.65%, and 56.17% at t=1 h, 2 h, 3 h, and 24 h, respectively. Hence, 1 h incubation was chosen as the optimium time required for maximum extraction, based on the extrapolation of the unknown concentration from the standard curve (Table 9).

Table 9: Summary of areas and percentages of recovery of RL71 and SMA-RL71 in plasma extracted with methanol. RL71 and SMA-RL71 were added to plasma and extracted with methanol at different time points, using 65% acetonitrile and 10 mM pH 5 acatate buffer as mobile phase. The percentage of recovery was calculated from the standard curve.

Compound	**Area (mAU*min)**	**% of recovery**
RL71 0.2 µg/500 µL	0.1478	-
SMA-RL71 0.2 µg/500 µL	0.1583	-
Extracted plasma with free drug (0.2 µg/500 µL, 1 h)	0.1094	57.63
Extracted plasma with micellar drug (0.2 µg/500 µL, 1 h)	0.1136	59.45
Extracted plasma with free drug (0.2 µg/500 µL, 2 h)	0.11	52.4
Extracted plasma with micellar drug (0.2 µg/500 µL, 2 h)	0.1037	54.4
Extracted plasma with free drug (0.2 µg/500 µL, 3 h)	0.1048	50.8
Extracted plasma with micellar drug (0.2 µg/500 µL, 3 h)	0.1113	55.65
Extracted plasma with free drug (0.2 µg/500 µL, 24 h)	0.0888	48.78
Extracted plasma with micellar drug (0.2 µg/500 µL, 24 h)	0.1067	56.17

3.2.3 Limit of Detection and Limit of Quantitation of RL71

Using the SNR, a value of 3 was obtained for RL71 dissolved in methanol, at a concentration between 10 to 20 ng/mL. Therefore, the LOD of RL71 is approximately between 10-20 ng/mL. Similarly, a value of 10 was obtained using the SNR at a concentration between 40 to 60 ng/mL. So, the LOQ for RL71 dissolved in methanol is approximately between 40 to 60 ng/mL. Hence, 40, 60, 80, and 200 ng/mL concentrations of RL71 were methanol extracted in plasma to determine the percentage of recovery. No signal was detected until 80 ng/mL. The recovery for 80 ng/mL in plasma was approximately 47% and 58% for 200 ng/mL (Table 10), respectively, when extrapolated from the standard curve.

Table 10: P**ercentage of recovery of RL71 in plasma subjected to methanol extraction.**

Compound	Area (mAU*min)	% of recovery
RL71 80 ng/mL	0.0206	-
RL71 200 ng/mL	0.1079	-
Extracted plasma with free drug (80 ng/mL, 1 h)	0.0058	47.12
Extracted plasma with free drug (200 ng/mL, 1 h)	0.0607	58.4

3.2.4 Surrogates for Plasma Extraction

Among the compounds screened, only five compounds (RL109, RL112, RL115, RL116, and RL117) had retention times that didn't overlap with RL71 and curcumin (Table 11). All the five compounds were then spiked with RL71 and curcumin to check if distinct peaks would be obtained. Only RL116 and RL112 showed good peak profiles. Hence, RL112 and RL116, along with RL71 were added to plasma, then methanol extracted, and spiked with 10 µL of 100 µg/mL curcumin. Only the plasma spiked with RL116 showed a peak along with RL71 and curcumin at their respective times (Figure 20). The recovery for RL116 was 40% and RL71 was 53%, based on the calculations from the standard curve. At this stage, RL116 is the best candidate as a surrogate for plasma extraction of RL71.

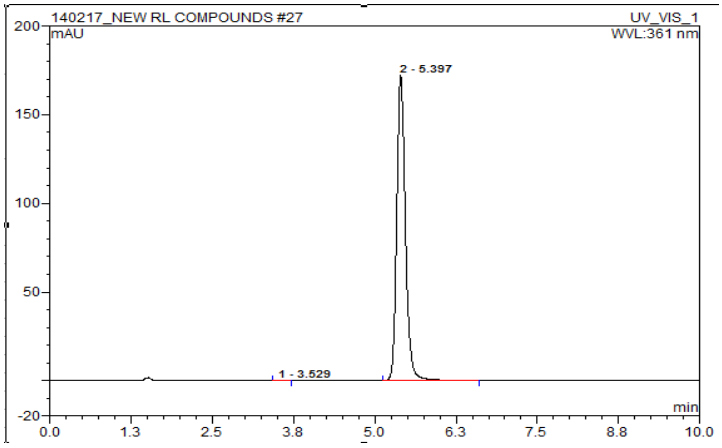

Figure 20: Chromatogram of RL116. RL116 at a concentration of 50 µg/mL was run using acetonitrile and 10 mM pH 5 acetate buffer as mobile phase. The retention time of RL116 was 5.4 min.

Table 11: **Summary of retention times of different compounds that could be used as a surrogate for plasma extraction of RL71.**

Compound	**Retention time (min)**
4-methoxybenzophenone	4.69
RL62	1.96
RL91	2.32
RL92	2.31
RL100	2.39
RL99	2.32
RL90	2.4
RL70	4.57
RL53	2.016
RL69	2.004
RL66	2.038
RL109	**5.888**
RL110	1.24, 6.63
RL112	**6.378**
RL113	4.486
RL114	2.913
RL115	**6.238**
RL116	**5.397**
RL117	**8.128, 9.327**
RL118	2.336
RL120	2.037
Raloxifene	2.016

Chapter Four: Discussion

4.1 Nanomicelle Formulation of RL71

The aim of the present study was to test if the micellar form of the most potent curcumin analogue, RL71, would be effective in eliciting tumour suppression in a xenograft model of triple negative breast cancer. Moreover, another aim of the study was optimisation of HPLC for the detection of RL71 in plasma, tumour, and tissues.

3, 5-bis (3, 4, 5-trimethoxybenzylidene)-1 methylpiperidin-4-one (RL71) is a second generation curcumin analogue synthesised in our laboratory as part of a series of 18 heterocyclic cyclohexanone analogues (Yadav *et al.* 2010). RL71 was the lead drug candidate with an IC_{50} value below of 0.3 µM in MDA-MB-231 cells and the ability to inhibit the activity of NFκB below 7.5 µM (Yadav *et al.*, 2010). Subsequently, RL71 was tested for cytotoxicity and mechanism of action in ER (-) breast cancer cell lines. RL71 (1 µM) elicited cell cycle arrest at the G2/M phase. In MDA-MB-231 cells, RL71 showed potent cytotoxicity, inhibited Akt phosphorylation and activated stress kinases. RL71 also demonstrated anti-angiogenic action in HUVEC cells by inhibiting its migration and ability to form tube-like structures. While RL71 (8.5 mg/kg) was orally bioavailable in female CD-1 mice, peak plasma concentrations were below the limit of detection by 2 h (Yadav *et al.*, 2012). It also failed to suppress tumour growth in a xenograft model of TNBC following 8.5 mg/kg given orally for 70 days (Yadav, 2012). Thus, RL71 showed potent anti-cancer activity *in vitro*, but failed to elicit tumour suppression in an animal model.

To overcome the problems associated with RL71 a novel drug delivery formulation was chosen. Micelles of styrene maleic acid co-polymers were used as a drug carrier because of their amphiphilic nature and ability to improve the pharmacokinetics of the drug. SMA micelles have been used previously to improve the pharmacokinetics of hydrophobic and toxic anti-cancer drugs such as pirarubicin (Greish *et al.*, 2005). Usage of SMA micelles to encapsulate such drugs greatly decreases the toxicity associated with the free drug and shows enhanced cytotoxic properties *in vitro* and tumour suppression in animal models (Greish *et al.*, 2005). Other examples of drug encapsulated using SMA micelles include doxorubicin (Greish *et al.*, 2004) and zinc protoporphyrin (Iyer *et al.*, 2007). Therefore, it was hypothesised that using SMA micelles to encapsulate RL71 would improve its bioavailability, anti-cancer properties, solubility and decrease the toxicity of the drug.

Different loadings of SMA-RL71 (5%, 10%, and 15%) were prepared and tested for its cytotoxic properties in MDA-MB-231 cell line. 15% SMA-RL71 demonstrated higher stability and cytotoxicity, slower release rate, and better internalisation (Taurin *et al.*, 2013). 15% SMA-RL71 was also cytotoxic in a tumour spheroid model (Taurin *et al.*, 2013). Tumour spheroids mimic the *in vivo* tumour architecture and hence can be used to predict the effect of a drug more accurately in an *in vitro* setting (Hirschhaeuser *et al.*, 2010). Thus, 15% SMA-RL71 demonstrated properties favourable for further evaluation as a drug for triple negative breast cancer in xenograft models.

4.2 Animal Models of Breast Cancer

Female SCID (2 to 2.5 months old) were used in this study to test the tumour - suppressive activity of SMA-RL71 because of the several advantageous properties they possess. The mice are named because of the homozygous mutation in the *scid* gene. This mutation impairs the development of T and B lymphocytes in the early stages of their lifespan (Bosma and Carroll, 1991). Thus, these mice are severely immunodeficient and readily accept engrafted cells such as human breast cancer cells when maintained in a specific-pathogen-free environment (Bosma and Carroll, 1991). The deficiency in the immune system of these mice is due to defects in the rearrangement of genes that encode antigen-specific receptors on B and T-cells (Schuler *et al.*, 1986). However, by 10 to 14 months of age, these mice start producing some functional B and T-cells; hence, younger mice are generally used in research to prevent rejection of xenograft (Bosma and Carroll, 1991). SCID mice are a better choice when compared to nude mice as nude mice lack only functional T-lymphocytes. They also have high levels of natural killer (NK) cells, lymphocyte-activated killer cells (LAK) and detectable levels of IgG and IgA, which act as a barrier in successful uptake of xenografts (Clarke, 1996). Moreover, the tumour uptake rate in these mice with regard to human breast cancer is low and metastasising capacity is also low, the main limiting factor being the site of tumour implantation (Price *et al.*, 1990, Price and Zhang, 1990). Injection of ER (-) breast cancer cell lines MDA-MB-231 and MDA-MB-435 into the mammary fat of these mice gave an uptake rate of 100%, whereas it was only 40% when injected subcutaneously (Price *et al.*, 1990).

MDA-MB-231 cells were used to inoculate female SCID mice as studies show that these cells have 100% uptake and form a good model for studying ER (-) breast cancer progression in animal models (Visonneau *et al.*, 1998). Inoculation of breast cancer cells into the flank of the mice was chosen as it is an established model used previously in our laboratory (Scandlyn *et al.*, 2008, Somers-Edgar *et al.*, 2008, Yadav *et al.*, 2012, Taurin *et al.*, 2013) as well as others (Shao *et al.*, 1998, Kawakami *et al.*, 2003, Laitem *et al.*, 2009). A Matrigel suspension of MDA-MB-231 cells was used as it enables better tumour growth due to the presence of several cell attachment molecules such as laminin, and fibronectin (Clarke, 1996, Dewan *et al.*, 2005).

4.3 In vivo Efficacy of SMA-RL71

To assess the efficacy of SMA-RL71, a dose response study was conducted initially. 5 mg/kg, 10 mg/kg and 15 mg/kg of the micellar drug (15% loading) and 10 mg/kg RL71 were chosen for this study. This was based on the results from previous studies that 8.5 mg/kg of free RL71 failed to suppress tumour growth (Yadav, 2012). Tail vein injections of the drug was used as this has been the established route of micellar drug administration in previous studies using different micellar drugs (Greish *et al.*, 2004, Greish *et al.*, 2005, Iyer *et al.*, 2007).

In the time course study using SMA-RL71 10 mg/kg, the mice were dosed with multiple injections for two weeks and three weeks. Interestingly, the mice dosed for two weeks exhibited better tumour suppression than those dosed for three weeks. The weight of the

tumours excised from the 3 weeks-treated mice were not statistically significant compared to control and also exhibited decreased statistically significant tumour suppression, compared to the 2 weeks-treated mice. This could be due to the drug becoming ineffective with prolonged administration. Development of drug resistance is one of the most common reasons for decreased response rates seen in the treatment of breast cancer (Liu *et al.*, 2008). Doxorubicin is one of the commonly used anti-cancer drug to treat breast cancer and resistance towards is one of the major reasons for therapy failure (Arafa el *et al.*, 2011). Some of the possible mechanisms by which the drug might have become ineffective are as follows: Activation of NFκB is an important factor responsible for induction of chemoresistance in many cancers, including breast cancer (Montagut *et al.*, 2006). In a study by Montagut *et al.*, the study of expression of NFκB in tumour specimens by immunohistochemistry from pre- and post-chemotherapy patients, treated with anthracycline- and/or taxane-containing neoadjuvant chemotherapy showed that in some patients, NFκB expression increased after chemotherapy (Montagut *et al.*, 2006). In doxorubicin- resistant breast cancer cells, nuclear translocation of p65 NFκB and its association with p300 histone acetylase led to suppression of p53 mediated apoptosis due to increased activity of the anti-apoptotic protein Bcl-2 (Sen *et al.*, 2011). In hepatocellular carcinoma HepG2 cells, treatment with curcumin led to drug resistance and decreased efficacy. Mechanistic studies revealed that the drug resistance was due to hypoxia-induced up-regulation of gene expression of multidrug resistance proteins ABCC1, ABCC2, and ABCC3 (Sakulterdkiat *et al.*, 2012). In melanoma cell line M14, treatment with 25 μM of curcumin had no significant anti-cancer effect. No inhibitory effect was observed on NFκB expression due to high expression of the cholesterol transporter and multidrug resistance gene ABCA1. Silencing of this drug transporter greatly improved the anti-cancer effects of curcumin due to the down-regulation of p65 NFκB, bcl-2 and survivin, thus leading to apoptosis (Bachmeier *et al.*, 2009). Cisplatin is a commonly used anti-cancer drug for many types of cancer such as ovarian, small-cell lung cancer, cervical and testicular cancer (Chauhan *et al.*, 2003). In cisplatin-resistant human epidermoid carcinoma cell line, reduced endocytosis of the drug and defective endosomal acidification were responsible for acquired cisplatin resistance (Chauhan *et al.*, 2003). Drug resistance can also be caused by ATP-dependent efflux of the drug due to the overexpression of ATP-binding cassette (ABC) transporters, such as ABCB1 (P-glycoprotein), ABCC1 (MRP1), and ABCG2 (breast cancer resistance protein, mitoxantrone resistance-associated protein) (Doyle *et al.*, 1998, Yang *et al.*, 2000, Gottesman *et al.*, 2002). Anti-cancer drugs can also become less effective due to detoxification by conjugation with glutathione, catalysed by GSTs and exported from the cells by glutathione conjugate export pump (Zhang *et al.*, 1998). Increased DNA repair is another mechanism by which anti-cancer drugs become ineffective because of the ability of the cancerous cell to repair the damage induced by the drug (Masuda *et al.*, 1988, Shirota *et al.*, 2001).

This is a novel study, as very few studies have encapsulated curcumin analogues, specifically for the treatment of breast cancer. An example of encapsulation of curcumin analogue to target breast cancer is the legumain-targeted liposomal form (Leg-HC-NPs) of the curcumin analogue hydrazinocurcumin (HC). *In vivo*, dosing of BALB/c female mice

after tumour induction, with multiple injections of Leg-HC-NPs (1 mM, one injection every 3 days for 15 days) significantly reduced the tumour volume (approximately 73%) compared with other treatment groups. This study supports the fact that encapsulation of curcumin analogue and multiple injections are more effective in achieving tumour suppression (Zhang *et al.*, 2013). This study cannot be directly compared as the study was more around the effects of macrophages on breast cancer cells. Nevertheless, it closely reflected the pattern of this study as the mice were subcutaneously injected with tumour cells and macrophages, treated with both the free and nano form of the drug and were sacrificed on day 30. Similar to our study, the encapsulated form of the drug was less toxic as free HC damaged the caudal vein and caused high mortality (3/5) in mice after five injections within 15 days. The authors postulated that the high mortality rate might also be due to the reduced biological action of HC (Zhang *et al.*, 2013).

There are other studies that have focussed on encapsulation of curcumin in nanoparticles to treat breast cancer. For example, Chun *et al* studied the effect of intraductal injections of NanoCurc in N-methyl-N-nitrosourea (MNU)-administered rats that develop mammary tumours approximately in six months post-MNU exposure. The study employed three treatment cycles of the free drug, and nano form injected intraductally, and also oral free curcumin (200 mg/kg). The NanoCurc delivered approximately 168 µg of curcumin per teat. The rats dosed intraductally with NanoCurc exhibited a significantly smaller mean tumour volume (Chun *et al.*, 2012). Thus, this study also emphasises the fact that multiple cycles of injection and encapsulation of the drug results in a better tumour suppression.

Tang *et al.* (2010) studied the effect of curcumin-oligo ethylene glycol (Cur-OEG) nanoparticles in BALB/c female nude mice injected with MDA-MB-468 cells and after the formation of 5 mm^3 palpable tumours, the mice received a single intravenous injection of 25 mg/kg of Cur-OEG nanoparticle. 48 h after treatment, there was a significant decrease (42%) in tumour weight, compared to the control group based on the average tumour weight (Tang *et al.*, 2010). In another study, BALB/c female nude mice were injected subcutaneously with a single dose of curcumin encapsulated in poly (lactic-co-glycolide) (containing 58.2 mg of curcumin) a day before the tumour inoculation with MDA-MB-231 cells. This resulted in a significant tumour suppression when the mice were sacrificed. Compared to the empty nanoparticle-treated mice, there was a 49% decrease in the mean tumour volume in the group treated with PLGA-curcumin nanoparticles (Shahani *et al.*, 2010). In a subcutaneous 4T1 breast tumour model using BALB/c mice, daily intravenous injection for 10 days of 30 mg/kg of polymeric micelles of curcumin showed a 76% reduction in tumour burden compared to control at the end of the study (Liu *et al.*, 2013).

Though the aforementioned studies used different strains of mice and study design, one thing that could be observed is that in almost all the studies the dose of curcumin nanoparticle used was much higher than what was used in this study for RL71 nanomicelle (10 mg/kg) and fewer injections (4 in total).

4.4 Effect of SMA-RL71 on Animal Health

All mice gained a similar amount of weight at the end of each study. However, the mice exhibited signs of toxicity such as increase in spleen, liver and kidney weight, and in the time course study, splenomegaly and liver discolouration were observed in the mice dosed with the micellar drug for three weeks.

Increased drug accumulation in the spleen is commonly observed in animals dosed with nanoformulations such as micelles, as it is one of the organs associated with the elimination of micelles from the body (Blanco *et al.*, 2010, Oberoi *et al.*, 2012). Intravenous administration of PLGA-curcumin nanoparticles in rats produced a significant accumulation of curcumin in the spleen and lung. The AUC for spleen was highest (1213 ± 102 min μg/mL). The increase in accumulation of the drug in the spleen was due to its phagocytic function (Tsai *et al.*, 2011). In an *in vivo* study using β-lapachone polymeric micelles in mice with non-small cell lung cancer, the largest accumulation of the micelles was found in spleen (Blanco *et al.*, 2010). Increase in spleen weight and histological changes in spleen, liver, kidney, and heart were observed in mice dosed intravenously with triptolide-loaded polymeric micelles (Xu *et al.*, 2013). However, the degree of pathological damage was lesser in the mice dosed with the micellar drug when compared to the free drug (Xu *et al.*, 2013). This might explain why an increase in spleen weight was observed in the mice dosed with SMA-RL71.

Curcumin on its own causes enlargement of spleen. A study by Chin *et al.* investigated the effect of dietary supplementation of curcumin on copper, iron and zinc status in C57BL/6J mice. The mice were fed a dietary supplementation containing 0.2% curcumin for 6 months. The mice fed with dietary curcumin exhibited a 40% increase in spleen mass. However, this was not associated with inflammation (Chin *et al.* 2014).

Pathak *et al.* studied the effects of herbal compounds including curcumin in splenocytes isolated from mice and treated with cadmium to induce immunotoxicity. Splenic cells were treated with either free cadmium or cadmium plus curcumin. The cells treated with cadmium plus curcumin exhibited increased cell viability, decreased ROS production and increased GSH levels, inhibition of mitochondrial pathway-mediated apoptosis, and increased secretion of cytokines such as IL-2 and IFN-γ. The authors postulated that the changes observed in splenic cells were due to the immunomodulatory effects elicited by curcumin (Pathak and Khandelwal, 2008). However, an increase in spleen weight was not observed in mice orally dosed daily with RL71 for 70 days (Yadav, 2012). SMA also has immune-stimulating properties such as macrophage, T-cell and natural killer cell activation (Oda *et al.*, 1986, Suzuki *et al.*, 1990).

The liver is another organ associated with increased drug accumulation due to its role in the clearance of nanodrugs (Blanco *et al.*, 2010). Increase in liver weight (2 weeks and 3 weeks treatment) and, liver decolourisation were observed in mice dosed with the micellar drug (10 mg/kg for 3 weeks). This suggests that the aforementioned dose caused liver damage.

To investigate if the increase in spleen and liver weight were associated with histological changes, histological analysis with hematoxylin and eosin (H&E) stain is suggested. Histological analysis of other organs, and plasma markers of liver and kidney toxicity such as ALT and creatinine are also suggested to rule out toxicity from SMA-RL71.

4.5 Optimisation of HPLC for the Detection of RL71

One of the important aims of the study was to develop a simple, sensitive and cost-effective method for the detection of RL71 along with an appropriate surrogate, by HPLC in plasma and tissues of mice dosed with SMA-RL71. It is important to study the biodistribution of the drug in various tissues to validate drug accumulation in tumour tissues via the EPR effect and assess the amount of drug delivered to major organs such as liver, kidneys, and spleen for signs of toxicity.

For the method development, an HPLC with UV/VIS PDA detector was used. Acetonitrile was chosen as the organic phase because, compared to other organic solvents such as methanol, acetonitrile has a high eluting capacity (Gugulothu *et al.*, 2013). For the method development, curcumin was chosen as an internal standard because of its structural similarity to RL71. It is important to use an internal standard to account for detection stability and to account for errors that might arise during sample injection. The surrogate (RL116) serves the purpose of accounting for the losses of the drug through the extraction process as it is structurally similar and expected to behave similarly to the compound of interest, and has minimal plasma binding properties. The detection wavelengths of RL71, RL116 and curcumin were 371, 383 and 425 nm, respectively.

Mobile phase optimisation was performed through several variations in the composition and conditions of the mobile phase to obtain the best chromatographic separation. An isocratic method was chosen as it produces minimal variation in column conditions, and is also simple, having fewer chances of producing baseline errors (Shah *et al.*, 2010). Acetonitrile and water were initially chosen as the mobile phase. Different percentages of acetonitrile such as 45, 55, 65, and 75 were tried, among which 65% acetonitrile and water as the mobile phase gave the best peak characteristics such as shape, height and sharpness. However, when RL71 and curcumin were run using 65% acetonitrile and water as the mobile phase, there was hardly (approximately 0.6 min) any retention time separation between the two compounds. Hence, it was decided to test a new mobile phase.

The structure and properties of curcumin require the presence of acetic acid for proper peak shape and elution (Gugulothu *et al.*, 2013). A simple, reliable method for quantitative detection of curcumin analogues containing the 1,5- diaryl- 3- oxo- 1,4- pentadienyl moiety has already been described using acetonitrile and 10 mM pH 5 acetate buffer as mobile phase (Singh *et al.*, 2010) and hence, it was adapted with slight modifications for method development. The new mobile phase was 65% acetonitrile and 10 mM pH 5 acetate buffer. The retention times of curcumin, RL71 and RL116 were 3.4, 4.5 and 5.5 min, respectively. This was obtained consistently and a calibration curve was built using different concentrations of RL71 and RL116.

For plasma extraction of RL71, the method optimised by Dr. Lesley Larsen of the Department of Chemistry was followed, with slight modifications. The method involved addition of the drug to a plasma sample, followed by incubation with methanol. Methanol was used to precipitate the protein present in the plasma as it is a routinely followed method (Ferrandi *et al.*, 1997, Teoh *et al.*, 2010). The plasma proteins if not removed, will interfere with the compound detection as they bind the drug and decrease the amount of free drug that can be analysed (Nikolin *et al.*, 2004). Different incubation periods (Table 9) were tested to determine if increasing the incubation period would lead to increased protein precipitation, and thus increase the recovery of the drug. However, 1 h incubation itself gave the maximum recovery. The recovery for RL71 and RL116 was 53% and 40%, respectively.

4.6 Conclusions/Future Directions

The tumour reduction obtained in xenograft models of TNBC with twice weekly injections for two weeks of SMA-RL71 10 mg/kg demonstrates that it is a potent anti-cancer drug. Since SMA-RL71 was successful in eliciting tumour suppression, it is assumed that its bioavailability is significantly higher compared to RL71. HPLC analysis of plasma, tumour and tissues is required to determine the drug accumulation. Future directions include testing the same dose in metastatic models of TNBC. This is important as most of the breast cancer patients die due to metastatic disease.

Preliminary toxicity studies from animal and organ weight show that SMA-RL71 elicited signs of toxicity such as increase in spleen, liver and kidney weight, and splenomegaly and liver discolouration. Toxicity studies such as plasma markers for liver, and kidney are required to clearly establish that it is indeed a safe drug. (Plasma ALT and creatinine values were subsequently determined to be in the normal range for all treatments: M.Nimick, personal communication) Histological examination of liver, kidney and spleen will help in ruling out damage to those organs, especially spleen, by SMA-RL71.

In vitro mechanisms of action of RL71 include modulation of the protein expression of EGFR, Akt, NFκB, mammalian target of rapamycin (mTOR), and stress kinases JNK1/2 and p38. It is expected that the expression of these proteins will also be modulated in the tumours of the mice dosed with SMA-RL71. To confirm, Western blot analysis of the tumours is suggested. Tumour suppression in animals is generally associated with decreased cell proliferation, increased apoptosis and decreased angiogenesis. To investigate the histological changes in tumours of the mice dosed with SMA-RL71, staining of the tumour tissues for Ki-67, active caspase-3 and CD105, which are markers of cell proliferation, apoptosis and microvessel density (MVD), should be performed. The results from immunohistochemistry (IHC) will give vital information about the ability of SMA-RL71 to modulate cell proliferation, apoptosis and angiogenesis.

References

Adams, B.K., Cai, J., Armstrong, J., Herold, M., Lu, Y.J., Sun, A., Snyder, J.P., Liotta, D.C., Jones, D.P. and Shoji, M. (2005). "EF24, a novel synthetic curcumin analog, induces apoptosis in cancer cells via a redox-dependent mechanism." Anticancer Drugs **16**(3): 263-275.

Adams, B.K., Ferstl, E.M., Davis, M.C., Herold, M., Kurtkaya, S., Camalier, R.F., Hollingshead, M.G., Kaur, G., Sausville, E.A., Rickles, F.R., Snyder, J.P., Liotta, D.C. and Shoji, M. (2004). "Synthesis and biological evaluation of novel curcumin analogs as anti-cancer and anti-angiogenesis agents." Bioorganic & Medicinal Chemistry **12**(14): 3871-3883.

Agashe, H., Lagisetty, P., Sahoo, K., Bourne, D., Grady, B. and Awasthi, V. (2011). "Liposome-encapsulated EF24-HPbetaCD inclusion complex: a preformulation study and biodistribution in a rat model." Journal of Nanoparticle Research **13**(6): 2609-2623.

Al-Hujaily, E.M., Mohamed, A.G., Al-Sharif, I., Youssef, K.M., Manogaran, P.S., Al-Otaibi, B., Al-Haza'a, A., Al-Jammaz, I., Al-Hussein, K. and Aboussekhra, A. (2011). "PAC, a novel curcumin analogue, has anti-breast cancer properties with higher efficiency on ER-negative cells." Breast Cancer Research and Treatment **128**(1): 97-107.

Anand, P., Thomas, S.G., Kunnumakkara, A.B., Sundaram, C., Harikumar, K.B., Sung, B., Tharakan, S.T., Misra, K., Priyadarsini, I.K., Rajasekharan, K.N. and Aggarwal, B.B. (2008). "Biological activities of curcumin and its analogues (Congeners) made by man and Mother Nature." Biochemical Pharmacology **76**(11): 1590-1611.

Arafa el, S.A., Zhu, Q., Shah, Z.I., Wani, G., Barakat, B.M., Racoma, I., El-Mahdy, M.A. and Wani, A.A. (2011). "Thymoquinone up-regulates PTEN expression and induces apoptosis in doxorubicin-resistant human breast cancer cells." Mutation Research **706**(1-2): 28-35.

Arnida, Janat-Amsbury, M.M., Ray, A., Peterson, C.M. and Ghandehari, H. (2011). "Geometry and surface characteristics of gold nanoparticles influence their biodistribution and uptake by macrophages." European Journal of Pharmaceutics and Biopharmaceutics **77**(3): 417-423.

Bachmeier, B., Iancu, C., Killian, P., Kronski, E., Mirisola, V., Angelini, G., Jochum, M., Nerlich, A. and Pfeffer, U. (2009). "Overexpression of the ATP binding cassette gene ABCA1 determines resistance to Curcumin in M14 melanoma cells." Molecular Cancer **8**(1): 1-12.

Bachmeier, B., Nerlich, A.G., Iancu, C.M., Cilli, M., Schleicher, E., Vene, R., Dell'Eva, R., Jochum, M., Albini, A. and Pfeffer, U. (2007). "The chemopreventive polyphenol Curcumin prevents hematogenous breast cancer metastases in immunodeficient mice." Cellular Physiology and Biochemistry **19**(1-4): 137-152.

Balogun, E., Hoque, M., Gong, P., Killeen, E., Green, C.J., Foresti, R., Alam, J. and Motterlini, R. (2003). "Curcumin activates the haem oxygenase-1 gene via regulation of Nrf2 and the antioxidant-responsive element." Biochemical Journal **371**(Pt 3): 887-895.

Blanco, E., Bey, E.A., Khemtong, C., Yang, S.G., Setti-Guthi, J., Chen, H., Kessinger, C.W., Carnevale, K.A., Bornmann, W.G., Boothman, D.A. and Gao, J. (2010). "Beta-lapachone micellar nanotherapeutics for non-small cell lung cancer therapy." Cancer Research **70**(10): 3896-3904.

Bosma, M.J. and Carroll, A.M. (1991). "The SCID mouse mutant: definition, characterization, and potential uses." Annual Review of Immunology **9**: 323-350.

Brouet, I. and Ohshima, H. (1995). "Curcumin, an anti-tumour promoter and anti-inflammatory agent, inhibits induction of nitric oxide synthase in activated macrophages." Biochemical and Biophysical Research Communications **206**(2): 533-540.

Carroll, C.E., Benakanakere, I., Besch-Williford, C., Ellersieck, M.R. and Hyder, S.M. (2010). "Curcumin delays development of medroxyprogesterone acetate-accelerated 7,12-dimethylbenz[a]anthracene-induced mammary tumors." Menopause **17**(1): 178-184.

Chakraborti, S., Dhar, G., Dwivedi, V., Das, A., Poddar, A., Chakraborti, G., Basu, G., Chakrabarti, P., Surolia, A. and Bhattacharyya, B. (2013). "Stable and Potent Analogues Derived from the Modification of the Dicarbonyl Moiety of Curcumin." Biochemistry **52**(42): 7449-7460.

Chauhan, S.S., Liang, X.J., Su, A.W., Pai-Panandiker, A., Shen, D.W., Hanover, J.A. and Gottesman, M.M. (2003). "Reduced endocytosis and altered lysosome function in cisplatin-resistant cell lines." British Journal of Cancer **88**(8): 1327-1334.

Chin, D., Huebbe, P., Frank, J., Rimbach, G. and Pallauf, K. (2014). "Curcumin may impair iron status when fed to mice for six months." Redox Biology **2**: 563-569.

Chun, Y.S., Bisht, S., Chenna, V., Pramanik, D., Yoshida, T., Hong, S.M., de Wilde, R.F., Zhang, Z., Huso, D.L., Zhao, M., Rudek, M.A., Stearns, V., Maitra, A. and Sukumar, S. (2012). "Intraductal administration of a polymeric nanoparticle formulation of curcumin (NanoCurc) significantly attenuates incidence of mammary tumors in a rodent chemical carcinogenesis model: Implications for breast cancer chemoprevention in at-risk populations." Carcinogenesis **33**(11): 2242-2249.

Clarke, R. (1996). "Human breast cancer cell line xenografts as models of breast cancer. The immunobiologies of recipient mice and the characteristics of several tumorigenic cell lines." Breast Cancer Research and Treatment **39**(1): 69-86.

Criscitiello, C., Azim, H.A., Jr., Schouten, P.C., Linn, S.C. and Sotiriou, C. (2012). "Understanding the biology of triple-negative breast cancer." Annals of Oncology **23 Suppl 6**: vi13-18.

Dent, R., Trudeau, M., Pritchard, K.I., Hanna, W.M., Kahn, H.K., Sawka, C.A., Lickley, L.A., Rawlinson, E., Sun, P. and Narod, S.A. (2007). "Triple-negative breast cancer: clinical features and patterns of recurrence." Clinical Cancer Research **13**(15 Pt 1): 4429-4434.

Dewan, M.Z., Terunuma, H., Ahmed, S., Ohba, K., Takada, M., Tanaka, Y., Toi, M. and Yamamoto, N. (2005). "Natural killer cells in breast cancer cell growth and metastasis in SCID mice." Biomedicine & Pharmacotherapy **59 Suppl 2**: S375-379.

Doyle, L.A., Yang, W., Abruzzo, L.V., Krogmann, T., Gao, Y., Rishi, A.K. and Ross, D.D. (1998). "A multidrug resistance transporter from human MCF-7 breast cancer cells." Proceedings of the National Academy of Sciences of the United States of America **95**(26): 15665-15670.

Duffy, M.J., McGowan, P.M. and Crown, J. (2012). "Targeted therapy for triple-negative breast cancer: where are we?" International Journal of Cancer **131**(11): 2471-2477.

Fang, J., Nakamura, H. and Maeda, H. (2011). "The EPR effect: Unique features of tumor blood vessels for drug delivery, factors involved, and limitations and augmentation of the effect." Advanced Drug Delivery Reviews **63**(3): 136-151.

Ferrandi, M., Manunta, P., Balzan, S., Hamlyn, J.M., Bianchi, G. and Ferrari, P. (1997). "Ouabain-like Factor Quantification in Mammalian Tissues and Plasma: Comparison of Two Independent Assays." Hypertension **30**(4): 886-896.

Fuchs, J.R., Pandit, B., Bhasin, D., Etter, J.P., Regan, N., Abdelhamid, D., Li, C., Lin, J. and Li, P.-K. (2009). "Structure–activity relationship studies of curcumin analogues." Bioorganic & Medicinal Chemistry Letters **19**(7): 2065-2069.

Gottesman, M.M., Fojo, T. and Bates, S.E. (2002). "Multidrug resistance in cancer: role of ATP-dependent transporters." Nature Reviews Cancer **2**(1): 48-58.

Greish, K. (2007). "Enhanced permeability and retention of macromolecular drugs in solid tumors: a royal gate for targeted anticancer nanomedicines." Journal of Drug Targeting **15**(7-8): 457-464.

Greish, K., Nagamitsu, A., Fang, J. and Maeda, H. (2005). "Copoly(styrene-maleic acid)-pirarubicin micelles: high tumor-targeting efficiency with little toxicity." Bioconjugate Chemistry **16**(1): 230-236.

Greish, K., Sawa, T., Fang, J., Akaike, T. and Maeda, H. (2004). "SMA-doxorubicin, a new polymeric micellar drug for effective targeting to solid tumours." Journal of Controlled Release **97**(2): 219-230.

Gugulothu, D., Desai, P. and Patravale, V. (2013). "A Versatile Liquid Chromatographic Technique for Pharmacokinetic Estimation of Curcumin in Human Plasma." Journal of Chromatographic Science 52(8): 872-879

Gupta, V., Aseh, A., Rios, C.N., Aggarwal, B.B. and Mathur, A.B. (2009). "Fabrication and characterization of silk fibroin-derived curcumin nanoparticles for cancer therapy." International Journal of Nanomedicine **4**: 115-122.

Hirschhaeuser, F., Menne, H., Dittfeld, C., West, J., Mueller-Klieser, W. and Kunz-Schughart, L.A. (2010). "Multicellular tumor spheroids: an underestimated tool is catching up again." Journal of Biotechnology **148**(1): 3-15.

Hudis, C.A. and Gianni, L. (2011). "Triple-negative breast cancer: an unmet medical need." Oncologist **16 Suppl 1**: 1-11.

Hutzen, B., Friedman, L., Sobo, M., Lin, L., Cen, L., De Angelis, S., Yamakoshi, H., Shibata, H., Iwabuchi, Y. and Lin, J. (2009). "Curcumin analogue GO-Y030 inhibits STAT3 activity and cell growth in breast and pancreatic carcinomas." International Journal of Oncology **35**(4): 867-872.

Iyer, A.K., Greish, K., Fang, J., Murakami, R. and Maeda, H. (2007). "High-loading nanosized micelles of copoly(styrene-maleic acid)-zinc protoporphyrin for targeted delivery of a potent heme oxygenase inhibitor." Biomaterials **28**(10): 1871-1881.

Iyer, A.K., Greish, K., Seki, T., Okazaki, S., Fang, J., Takeshita, K. and Maeda, H. (2007). "Polymeric micelles of zinc protoporphyrin for tumor targeted delivery based on EPR effect and singlet oxygen generation." Journal of Drug Targeting **15**(7-8): 496-506.

Jiang, M., Huang, O., Zhang, X., Xie, Z., Shen, A., Liu, H., Geng, M. and Shen, K. (2013). "Curcumin induces cell death and restores tamoxifen sensitivity in the antiestrogen-resistant breast cancer cell lines MCF-7/LCC2 and MCF-7/LCC9." Molecules **18**(1): 701-720.

Kawakami, K., Kawakami, M., Husain, S.R. and Puri, R.K. (2003). "Effect of interleukin (IL)-4 cytotoxin on breast tumor growth after in vivo gene transfer of IL-4 receptor alpha chain." Clinical Cancer Research **9**(5): 1826-1836.

Kennecke, H., Yerushalmi, R., Woods, R., Cheang, M.C., Voduc, D., Speers, C.H., Nielsen, T.O. and Gelmon, K. (2010). "Metastatic behavior of breast cancer subtypes." Journal of Clinical Oncology **28**(20): 3271-3277.

Kurien, B.T., Singh, A., Matsumoto, H. and Scofield, R.H. (2007). "Improving the solubility and pharmacological efficacy of curcumin by heat treatment." Assay and Drug Development Technologies **5**(4): 567-576.

Lai, H.W., Chien, S.Y., Kuo, S.J., Tseng, L.M., Lin, H.Y., Chi, C.W. and Chen, D.R. (2012). "The Potential Utility of Curcumin in the Treatment of HER-2-Overexpressed Breast Cancer: An In Vitro and In Vivo Comparison Study with Herceptin." Evidence-Based Complementary and Alternative Medicine **2012**: 486568.

Laitem, C., Leprivier, G., Choul-Li, S., Begue, A., Monte, D., Larsimont, D., Dumont, P., Duterque-Coquillaud, M. and Aumercier, M. (2009). "Ets-1 p27: a novel Ets-1 isoform with dominant-negative effects on the transcriptional properties and the subcellular localization of Ets-1 p51." Oncogene **28**(20): 2087-2099.

Lee, D.S., Lee, M.K. and Kim, J.H. (2009). "Curcumin Induces Cell Cycle Arrest and Apoptosis in Human Osteosarcoma (HOS) Cells." Anticancer Research **29**(12): 5039-5044.

Leung, E., Rewcastle, G., Joseph, W., Rosengren, R., Larsen, L. and Baguley, B. (2012). "Identification of cyclohexanone derivatives that act as catalytic inhibitors of topoisomerase I: effects on tamoxifen-resistant MCF-7 cancer cells." Investigational New Drugs **30**(6): 2103-2112.

Li, S.-D. and Huang, L. (2008). "Pharmacokinetics and Biodistribution of Nanoparticles." Molecular Pharmaceutics **5**(4): 496-504.

Liang, G., Shao, L., Wang, Y., Zhao, C., Chu, Y., Xiao, J., Zhao, Y., Li, X. and Yang, S. (2009). "Exploration and synthesis of curcumin analogues with improved structural stability both in vitro and in vivo as cytotoxic agents." Bioorganic & Medicinal Chemistry **17**(6): 2623-2631.

Liedtke, C., Mazouni, C., Hess, K.R., Andre, F., Tordai, A., Mejia, J.A., Symmans, W.F., Gonzalez-Angulo, A.M., Hennessy, B., Green, M., Cristofanilli, M., Hortobagyi, G.N. and Pusztai, L. (2008). "Response to neoadjuvant therapy and long-term survival in patients with triple-negative breast cancer." Journal of Clinical Oncology **26**(8): 1275-1281.

Lin, C.-C., Lu, Y.-P., Lou, Y.-R., Ho, C.-T., Newmark, H.H., MacDonald, C., Singletary, K.W. and Huang, M.-T. (2001). "Inhibition by dietary dibenzoylmethane of mammary gland proliferation, formation of DMBA–DNA adducts in mammary glands, and mammary tumorigenesis in Sencar mice." Cancer Letters **168**(2): 125-132.

Lin, C.C., Ho, C.T. and Huang, M.T. (2001). "Mechanistic studies on the inhibitory action of dietary dibenzoylmethane, a beta-diketone analogue of curcumin, on 7,12-dimethylbenz[a]anthracene-induced mammary tumorigenesis." Proceedings of the National Science Council, Republic of China. Part B **25**(3): 158-165.

Lin, L., Hutzen, B., Ball, S., Foust, E., Sobo, M., Deangelis, S., Pandit, B., Friedman, L., Li, C., Li, P.-K., Fuchs, J. and Lin, J. (2009). "New curcumin analogues exhibit enhanced growth-suppressive activity and inhibit AKT and signal transducer and activator of transcription 3 phosphorylation in breast and prostate cancer cells." Cancer Science **100**(9): 1719-1727.

Liu, H., Liu, Y. and Zhang, J.T. (2008). "A new mechanism of drug resistance in breast cancer cells: fatty acid synthase overexpression-mediated palmitate overproduction." Molecular Cancer Therapeutics **7**(2): 263-270.

Liu, L., Sun, L., Wu, Q., Guo, W., Li, L., Chen, Y., Li, Y., Gong, C., Qian, Z. and Wei, Y. (2013). "Curcumin loaded polymeric micelles inhibit breast tumor growth and spontaneous pulmonary metastasis." International Journal of Pharmaceutics **443**(1–2): 175-182.

Logan-Smith, M.J., Lockyer, P.J., East, J.M. and Lee, A.G. (2001). "Curcumin, a molecule that inhibits the Ca2+-ATPase of sarcoplasmic reticulum but increases the rate of accumulation of Ca2+." Journal of Biological Chemistry **276**(50): 46905-46911.

Maeda, H., Ueda, M., Morinaga, T. and Matsumoto, T. (1985). "Conjugation of poly(styrene-co-maleic acid) derivatives to the antitumor protein neocarzinostatin: pronounced improvements in pharmacological properties." Journal of Medicinal Chemistry **28**(4): 455-461.

Masuda, H., Ozols, R.F., Lai, G.M., Fojo, A., Rothenberg, M. and Hamilton, T.C. (1988). "Increased DNA repair as a mechanism of acquired resistance to cis-diamminedichloroplatinum (II) in human ovarian cancer cell lines." Cancer Research **48**(20): 5713-5716.

Masuelli, L., Benvenuto, M., Fantini, M., Marzocchella, L., Sacchetti, P., Di Stefano, E., Tresoldi, I., Izzi, V., Bernardini, R., Palumbo, C., Mattei, M., Lista, F., Galvano, F., Modesti, A. and Bei, R. (2013). "Curcumin induces apoptosis in breast cancer cell lines and delays the growth of mammary tumors in neu transgenic mice." Journal of Biological Regulators & Homeostatic Agents **27**(1): 105-119.

Menon, V.P. and Sudheer, A.R. (2007). "Antioxidant and anti-inflammatory properties of curcumin." Advances in Experimental Medicine and Biology **595**: 105-125.

Miller, J.M. (2009). Quantitation: Detectors and Methods. Chromatography, John Wiley & Sons, Inc.**:** 277-307.

Moghimi, S.M., Hunter, A.C. and Murray, J.C. (2001). "Long-circulating and target-specific nanoparticles: theory to practice." Pharmacological Reviews **53**(2): 283-318.

Montagut, C., Tusquets, I., Ferrer, B., Corominas, J.M., Bellosillo, B., Campas, C., Suarez, M., Fabregat, X., Campo, E., Gascon, P., Serrano, S., Fernandez, P.L., Rovira, A. and Albanell, J. (2006). "Activation of nuclear factor-kappa B is linked to resistance to neoadjuvant chemotherapy in breast cancer patients." Endocrine-Related Cancer **13**(2): 607-616.

Mosley, C., Liotta, D. and Snyder, J. (2007). HIGHLY ACTIVE ANTICANCER CURCUMIN ANALOGUES. The Molecular Targets and Therapeutic Uses of Curcumin in Health and Disease. B. Aggarwal, Y.-J. Surh and S. Shishodia, Springer US. **595:** 77-103.

Mukerjee, A. and Vishwanatha, J.K. (2009). "Formulation, characterization and evaluation of curcumin-loaded PLGA nanospheres for cancer therapy." Anticancer Research **29**(10): 3867-3875.

New Zealand Breast Cancer Foundation (2011). "Breast Cancer in New Zealand. In: nzbcf.org.nz [Internet].".Retrieved Mar 03, 2014, from http://www.nzbcf.org.nz/Portals/0/Documents/bhe_kit_2011_breast_cancer_facts_in_nz_april_final.pdf.

Nikolin, B., Imamovic, B., Medanhodzic-Vuk, S. and Sober, M. (2004). "High perfomance liquid chromatography in pharmaceutical analyses." Bosnian Journal of Basic Medical Sciences **4**(2): 5-9.

Noguchi, Y., Wu, J., Duncan, R., Strohalm, J., Ulbrich, K., Akaike, T. and Maeda, H. (1998). "Early phase tumor accumulation of macromolecules: a great difference in clearance rate between tumor and normal tissues." Japanese Journal of Cancer Research **89**(3): 307-314.

Oberoi, H.S., Nukolova, N.V., Laquer, F.C., Poluektova, L.Y., Huang, J., Alnouti, Y., Yokohira, M., Arnold, L.L., Kabanov, A.V., Cohen, S.M. and Bronich, T.K. (2012). "Cisplatin-loaded core cross-linked micelles: comparative pharmacokinetics, antitumor activity, and toxicity in mice." International Journal of Nanomedicine **7**: 2557-2571.

Oda, T., Morinaga, T. and Maeda, H. (1986). "Stimulation of macrophage by polyanions and its conjugated proteins and effect on cell membrane." Proceedings of the Society for Experimental Biology and Medicine **181**(1): 9-17.

Ohori, H., Yamakoshi, H., Tomizawa, M., Shibuya, M., Kakudo, Y., Takahashi, A., Takahashi, S., Kato, S., Suzuki, T., Ishioka, C., Iwabuchi, Y. and Shibata, H. (2006). "Synthesis and biological analysis of new curcumin analogues bearing an enhanced potential for the medicinal treatment of cancer." Molecular Cancer Therapeutics **5**(10): 2563-2571.

Padhye, S., Chavan, D., Pandey, S., Deshpande, J., Swamy, K.V. and Sarkar, F.H. (2010). "Perspectives on chemopreventive and therapeutic potential of curcumin analogs in medicinal chemistry." Mini Reviews in Medicinal Chemistry **10**(5): 372-387.

Pan, M.H., Huang, T.M. and Lin, J.K. (1999). "Biotransformation of curcumin through reduction and glucuronidation in mice." Drug Metabolism and Disposition **27**(4): 486-494.

Pathak, N. and Khandelwal, S. (2008). "Comparative efficacy of piperine, curcumin and picroliv against Cd immunotoxicity in mice." Biometals **21**(6): 649-661.

Perkins, S., Verschoyle, R.D., Hill, K., Parveen, I., Threadgill, M.D., Sharma, R.A., Williams, M.L., Steward, W.P. and Gescher, A.J. (2002). "Chemopreventive efficacy and pharmacokinetics of curcumin in the min/+ mouse, a model of familial adenomatous polyposis." Cancer Epidemiology, Biomarkers & Prevention **11**(6): 535-540.

Pervez, S., Khan, M.N. and Nasir, M.I. (2007). "Comparative predictive value of three prognostic markers--S-phase fraction, PCNA and Mitotic count on axillary lymph node metastasis in carcinoma breast." Journal of Ayub Medical College Abbottabad **19**(1): 3-5.

Petrangeli, E., Lubrano, C., Ortolani, F., Ravenna, L., Vacca, A., Sciacchitano, S., Frati, L. and Gulino, A. (1994). "Estrogen receptors: new perspectives in breast cancer management." The Journal of Steroid Biochemistry and Molecular Biology **49**(4-6): 327-331.

Petros, R.A. and DeSimone, J.M. (2010). "Strategies in the design of nanoparticles for therapeutic applications." Nature Reviews Drug Discovery **9**(8): 615-627.

Price, J.E., Polyzos, A., Zhang, R.D. and Daniels, L.M. (1990). "Tumorigenicity and metastasis of human breast carcinoma cell lines in nude mice." Cancer Research **50**(3): 717-721.

Price, J.E. and Zhang, R.D. (1990). "Studies of human breast cancer metastasis using nude mice." Cancer and Metastasis Reviews **8**(4): 285-297.

Rakha, E.A., Reis-Filho, J.S. and Ellis, I.O. (2008). "Basal-Like Breast Cancer: A Critical Review." Journal of Clinical Oncology **26**(15): 2568-2581.

Ravindranath, V. and Chandrasekhara, N. (1980). "Absorption and tissue distribution of curcumin in rats." Toxicology **16**(3): 259-265.

Rhee, J., Han, S.W., Oh, D.Y., Kim, J.H., Im, S.A., Han, W., Park, I.A., Noh, D.Y., Bang, Y.J. and Kim, T.Y. (2008). "The clinicopathologic characteristics and prognostic significance of triple-negativity in node-negative breast cancer." BMC Cancer **8**: 307.

Robertson, J.F. (1996). "Oestrogen receptor: a stable phenotype in breast cancer." British Journal of Cancer **73**(1): 5-12.

Rowe, D.L., Ozbay, T., O'Regan, R.M. and Nahta, R. (2009). "Modulation of the BRCA1 Protein and Induction of Apoptosis in Triple Negative Breast Cancer Cell Lines by the Polyphenolic Compound Curcumin." Breast Cancer: Basic and Clinical Research **3**: 61-75.

Sakulterdkiat, T., Srisomsap, C., Udomsangpetch, R., Svasti, J. and Lirdprapamongkol, K. (2012). "Curcumin resistance induced by hypoxia in HepG2 cells is mediated by multidrug-resistance-associated proteins." Anticancer Research **32**(12): 5337-5342.

Sandhu, R., Parker, J.S., Jones, W.D., Livasy, C.A. and Coleman, W.B. (2010). "Microarray-Based Gene Expression Profiling for Molecular Classification of Breast Cancer and Identification of New Targets for Therapy." Lab Medicine **41**(6): 364-372.

Sandur, S.K., Pandey, M.K., Sung, B., Ahn, K.S., Murakami, A., Sethi, G., Limtrakul, P., Badmaev, V. and Aggarwal, B.B. (2007). "Curcumin, demethoxycurcumin, bisdemethoxycurcumin, tetrahydrocurcumin and turmerones differentially regulate anti-inflammatory and anti-proliferative responses through a ROS-independent mechanism." Carcinogenesis **28**(8): 1765-1773.

Scandlyn, M.J., Stuart, E.C., Somers-Edgar, T.J., Menzies, A.R. and Rosengren, R.J. (2008). "A new role for tamoxifen in oestrogen receptor-negative breast cancer when it is combined with epigallocatechin gallate." British Journal of Cancer **99**(7): 1056-1063.

Schneider, B.P., Winer, E.P., Foulkes, W.D., Garber, J., Perou, C.M., Richardson, A., Sledge, G.W. and Carey, L.A. (2008). "Triple-negative breast cancer: risk factors to potential targets." Clinical Cancer Research **14**(24): 8010-8018.

Schuler, W., Weiler, I.J., Schuler, A., Phillips, R.A., Rosenberg, N., Mak, T.W., Kearney, J.F., Perry, R.P. and Bosma, M.J. (1986). "Rearrangement of antigen receptor genes is defective in mice with severe combined immune deficiency." Cell **46**(7): 963-972.

Sen, G.S., Mohanty, S., Hossain, D.M., Bhattacharyya, S., Banerjee, S., Chakraborty, J., Saha, S., Ray, P., Bhattacharjee, P., Mandal, D., Bhattacharya, A., Chattopadhyay, S., Das, T. and Sa, G. (2011). "Curcumin enhances the efficacy of chemotherapy by tailoring p65NFkappaB-p300 cross-talk in favor of p53-p300 in breast cancer." Journal of Biological Chemistry **286**(49): 42232-42247.

Shah, S., Dhanani, T. and Kumar, S. (2013). "Validated HPLC method for identification and quantification of p-hydroxy benzoic acid and agnuside in Vitex negundo and Vitex trifolia." Journal of Pharmaceutical Analysis **3**(6): 500-508.

Shah, U.M., Patel, S.M., Patel, P.H., Hingorani, L. and Jadhav, R.B. (2010). "Development and Validation of a Simple Isocratic HPLC Method for Simultaneous Estimation of Phytosterols in Cissus quadrangularis." Indian Journal of Pharmaceutical Sciences **72**(6): 753-758.

Shahani, K., Swaminathan, S.K., Freeman, D., Blum, A., Ma, L. and Panyam, J. (2010). "Injectable sustained release microparticles of curcumin: a new concept for cancer chemoprevention." Cancer Research **70**(11): 4443-4452.

Shao, Z.M., Shen, Z.Z., Liu, C.H., Sartippour, M.R., Go, V.L., Heber, D. and Nguyen, M. (2002). "Curcumin exerts multiple suppressive effects on human breast carcinoma cells." International Journal of Cancer **98**(2): 234-240.

Shao, Z.M., Wu, J., Shen, Z.Z. and Barsky, S.H. (1998). "Genistein exerts multiple suppressive effects on human breast carcinoma cells." Cancer Research **58**(21): 4851-4857.

Shim, J.S., Kim, D.H., Jung, H.J., Kim, J.H., Lim, D., Lee, S.-K., Kim, K.-W., Ahn, J.W., Yoo, J.-S., Rho, J.-R., Shin, J. and Kwon, H.J. (2002). "Hydrazinocurcumin, a novel synthetic curcumin derivative, is a potent inhibitor of endothelial cell proliferation." Bioorganic & Medicinal Chemistry **10**(9): 2987-2992.

Shirota, Y., Stoehlmacher, J., Brabender, J., Xiong, Y.P., Uetake, H., Danenberg, K.D., Groshen, S., Tsao-Wei, D.D., Danenberg, P.V. and Lenz, H.J. (2001). "ERCC1 and thymidylate synthase mRNA levels predict survival for colorectal cancer patients receiving combination oxaliplatin and fluorouracil chemotherapy." Journal of Clinical Oncology **19**(23): 4298-4304.

Shoba, G., Joy, D., Joseph, T., Majeed, M., Rajendran, R. and Srinivas, P.S. (1998). "Influence of piperine on the pharmacokinetics of curcumin in animals and human volunteers." Planta Medica **64**(4): 353-356.

Shoji, M., Sun, A., Kisiel, W., Lu, Y.J., Shim, H., McCarey, B.E., Nichols, C., Parker, E.T., Pohl, J., Mosley, C.A., Alizadeh, A.R., Liotta, D.C. and Snyder, J.P. (2008). "Targeting tissue factor-expressing tumor angiogenesis and tumors with EF24 conjugated to factor VIIa." Journal of Drug Targeting **16**(3): 185-197.

Singh, R.S., Das, U., Dimmock, J.R. and Alcorn, J. (2010). "A general HPLC-UV method for the quantitative determination of curcumin analogues containing the 1,5-diaryl-3-oxo-1,4-pentadienyl pharmacophore in rat biomatrices." Journal of Chromatography. B, Analytical Technologies in the Biomedical and Life Sciences **878**(28): 2796-2802.

Singh, S.V., Hu, X., Srivastava, S.K., Singh, M., Xia, H., Orchard, J.L. and Zaren, H.A. (1998). "Mechanism of inhibition of benzo[a]pyrene-induced forestomach cancer in mice by dietary curcumin." Carcinogenesis **19**(8): 1357-1360.

Somers-Edgar, T., Taurin, S., Larsen, L., Chandramouli, A., Nelson, M. and Rosengren, R. (2011). "Mechanisms for the activity of heterocyclic cyclohexanone curcumin derivatives in estrogen receptor negative human breast cancer cell lines." Investigational New Drugs **29**(1): 87-97.

Somers-Edgar, T.J., Scandlyn, M.J., Stuart, E.C., Le Nedelec, M.J., Valentine, S.P. and Rosengren, R.J. (2008). "The combination of epigallocatechin gallate and curcumin suppresses ER alpha-breast cancer cell growth in vitro and in vivo." International Journal of Cancer **122**(9): 1966-1971.

Sørlie, T., Perou, C.M., Tibshirani, R., Aas, T., Geisler, S., Johnsen, H., Hastie, T., Eisen, M.B., van de Rijn, M., Jeffrey, S.S., Thorsen, T., Quist, H., Matese, J.C., Brown, P.O., Botstein, D., Lønning, P.E. and Børresen-Dale, A.-L. (2001). "Gene expression patterns of

breast carcinomas distinguish tumor subclasses with clinical implications." Proceedings of the National Academy of Sciences **98**(19): 10869-10874.

Stuart, E.C., Jarvis, R.M. and Rosengren, R.J. (2010). "In vitro mechanism of action for the cytotoxicity elicited by the combination of epigallocatechin gallate and raloxifene in MDA-MB-231 cells." Oncology Reports **24**(3): 779-785.

Suzuki, F., Pollard, R.B., Uchimura, S., Munakata, T. and Maeda, H. (1990). "Role of natural killer cells and macrophages in the nonspecific resistance to tumors in mice stimulated with SMANCS, a polymer-conjugated derivative of neocarzinostatin." Cancer Research **50**(13): 3897-3904.

Tang, H., Murphy, C.J., Zhang, B., Shen, Y., Sui, M., Van Kirk, E.A., Feng, X. and Murdoch, W.J. (2010). "Amphiphilic curcumin conjugate-forming nanoparticles as anticancer prodrug and drug carriers: in vitro and in vivo effects." Nanomedicine (London) **5**(6): 855-865.

Taurin, S., Allen, K.M., Scandlyn, M.J. and Rosengren, R.J. (2013). "Raloxifene reduces triple-negative breast cancer tumor growth and decreases EGFR expression." International Journal of Oncology **43**(3): 785-792.

Taurin, S., Nehoff, H., Diong, J., Larsen, L., Rosengren, R.J. and Greish, K. (2013). "Curcumin-derivative nanomicelles for the treatment of triple negative breast cancer." Journal of Drug Targeting **21**(7): 675-683.

Teoh, M., Narayanan, P., Moo, K.S., Radhakrisman, S., Pillappan, R., Bukhari, N.I. and Segarra, I. (2010). "HPLC determination of imatinib in plasma and tissues after multiple oral dose administration to mice." Pakistan Journal of Pharmaceutical Sciences **23**(1): 35-41.

Thangapazham, R.L., Sharma, A. and Maheshwari, R.K. (2006). "Multiple molecular targets in cancer chemoprevention by curcumin." The AAPS Journal **8**(3): E443-449.

Thomas, S.L., Zhong, D., Zhou, W., Malik, S., Liotta, D., Snyder, J.P., Hamel, E. and Giannakakou, P. (2008). "EF24, a novel curcumin analog, disrupts the microtubule cytoskeleton and inhibits HIF-1." Cell Cycle **7**(15): 2409-2417.

Tønnesen, H. and Karlsen, J. (1985). "Studies on curcumin and curcuminoids." Zeitschrift für Lebensmittel-Untersuchung und Forschung **180**(5): 402-404.

Tønnesen, H.H., Másson, M. and Loftsson, T. (2002). "Studies of curcumin and curcuminoids. XXVII. Cyclodextrin complexation: solubility, chemical and photochemical stability." International Journal of Pharmaceutics **244**(1–2): 127-135.

Tran, B. and Bedard, P.L. (2011). "Luminal-B breast cancer and novel therapeutic targets." Breast Cancer Research **13**(6): 221.

Tsai, Y.M., Chien, C.F., Lin, L.C. and Tsai, T.H. (2011). "Curcumin and its nano-formulation: the kinetics of tissue distribution and blood-brain barrier penetration." International Journal of Pharmaceutics **416**(1): 331-338.

Uney, K., Altan, F. and Elmas, M. (2011). "Development and validation of a high-performance liquid chromatography method for determination of cefquinome concentrations in sheep plasma and its application to pharmacokinetic studies." Antimicrobial Agents and Chemotherapy **55**(2): 854-859.

Verma, S.P., Salamone, E. and Goldin, B. (1997). "Curcumin and Genistein, Plant Natural Products, Show Synergistic Inhibitory Effects on the Growth of Human Breast Cancer MCF-7 Cells Induced by Estrogenic Pesticides." Biochemical and Biophysical Research Communications **233**(3): 692-696.

Visonneau, S., Cesano, A., Torosian, M.H., Miller, E.J. and Santoli, D. (1998). "Growth characteristics and metastatic properties of human breast cancer xenografts in immunodeficient mice." The American Journal of Pathology **152**(5): 1299-1311.

Wahlström, B. and Blennow, G. (1978). "A Study on the Fate of Curcumin in the Rat." Acta Pharmacologica et Toxicologica **43**(2): 86-92.

Wang, X., Zhang, Y., Zhang, X., Tian, W., Feng, W. and Chen, T. (2012). "The curcumin analogue hydrazinocurcumin exhibits potent suppressive activity on carcinogenicity of breast cancer cells via STAT3 inhibition." International Journal of Oncology **40**(4): 1189-1195.

Woo, H.B., Eom, Y.W., Park, K.-S., Ham, J., Ahn, C.M. and Lee, S. (2012). "Synthesis of substituted benzimidazolyl curcumin mimics and their anticancer activity." Bioorganic & Medicinal Chemistry Letters **22**(2): 933-936.

Wu, J., Akaike, T. and Maeda, H. (1998). "Modulation of enhanced vascular permeability in tumors by a bradykinin antagonist, a cyclooxygenase inhibitor, and a nitric oxide scavenger." Cancer Research **58**(1): 159-165.

Xu, L., Qiu, Y., Xu, H., Ao, W., Lam, W. and Yang, X. (2013). "Acute and subacute toxicity studies on triptolide and triptolide-loaded polymeric micelles following intravenous administration in rodents." Food and Chemical Toxicology **57**: 371-379.

Yadav, B., Taurin, S., Larsen, L. and Rosengren, R.J. (2012). "RL66 a second-generation curcumin analog has potent in vivo and in vitro anticancer activity in ERnegative breast cancer models." International Journal of Oncology **41**(5): 1723-1732.

Yadav, B., Taurin, S., Larsen, L. and Rosengren, R.J. (2012). "RL71, a second-generation curcumin analog, induces apoptosis and downregulates Akt in ER-negative breast cancer cells." International Journal of Oncology **41**(3): 1119-1127.

Yadav, B., Taurin, S., Rosengren, R.J., Schumacher, M., Diederich, M., Somers-Edgar, T.J. and Larsen, L. (2010). "Synthesis and cytotoxic potential of heterocyclic cyclohexanone analogues of curcumin." Bioorganic & Medicinal Chemistry **18**(18): 6701-6707.

Yadav, B., Taurin, S., Rosengren, R.J., Schumacher, M., Diederich, M., Somers-Edgar, T.J. and Larsen, L. (2010). "Synthesis and cytotoxic potential of heterocyclic cyclohexanone analogues of curcumin." Bioorganic & Medicinal Chemistry **18**(18): 6701-6707.

Yadav, B.D. (2012). Study of New Curcumin Analogs for the Treatment of Erα Negative Breast Cancers. , University of Otago. (Thesis, Doctor of Philosophy). Retrieved from **http://hdl.handle.net/10523/2290**.

Yallapu, M.M., Gupta, B.K., Jaggi, M. and Chauhan, S.C. (2010). "Fabrication of curcumin encapsulated PLGA nanoparticles for improved therapeutic effects in metastatic cancer cells." Journal of Colloid and Interface Science **351**(1): 19-29.

Yallapu, M.M., Jaggi, M. and Chauhan, S.C. (2013). "Curcumin nanomedicine: a road to cancer therapeutics." Current Pharmaceutical Design **19**(11): 1994-2010.

Yallapu, M.M., Maher, D.M., Sundram, V., Bell, M.C., Jaggi, M. and Chauhan, S.C. (2010). "Curcumin induces chemo/radio-sensitization in ovarian cancer cells and curcumin nanoparticles inhibit ovarian cancer cell growth." Journal of Ovarian Research **3**: 11.

Yang, C.H., Schneider, E., Kuo, M.L., Volk, E.L., Rocchi, E. and Chen, Y.C. (2000). "BCRP/MXR/ABCP expression in topotecan-resistant human breast carcinoma cells." Biochemical Pharmacology **60**(6): 831-837.

Yang, K.Y., Lin, L.C., Tseng, T.Y., Wang, S.C. and Tsai, T.H. (2007). "Oral bioavailability of curcumin in rat and the herbal analysis from Curcuma longa by LC-MS/MS." Journal of Chromatography. B, Analytical Technologies in the Biomedical and Life Sciences **853**(1-2): 183-189.

Youssef, K.M. and El-Sherbeny, M.A. (2005). "Synthesis and Antitumor Activity of Some Curcumin Analogs." Archiv der Pharmazie **338**(4): 181-189.

Yuan, F. (1998). "Transvascular drug delivery in solid tumors." Seminars in Radiation Oncology **8**(3): 164-175.

Zhang, J., Wang, Y., Yin, Q., Zhang, W., Zhang, T. and Niu, Y. (2013). "An associated classification of triple negative breast cancer: the risk of relapse and the response to chemotherapy." International Journal of Clinical and Experimental Pathology **6**(7): 1380-1391.

Zhang, K., Mack, P. and Wong, K.P. (1998). "Glutathione-related mechanisms in cellular resistance to anticancer drugs." International Journal of Oncology **12**(4): 871-882.

Zhang, X., Tian, W., Cai, X., Wang, X., Dang, W., Tang, H., Cao, H., Wang, L. and Chen, T. (2013). "Hydrazinocurcumin Encapsuled nanoparticles "re-educate" tumor-associated macrophages and exhibit anti-tumor effects on breast cancer following STAT3 suppression." PLoS One **8**(6): e65896.

Curriculum Vitae

Book Chapter:

Sundararajan, V., Rosengren, R.J., Greish, K. (2014). Curcumin analogues for the treatment of breast cancer revisited - the nanotechnology approach. In Pouliquen, D.L. (Ed.), *Curcumin: Synthesis, Emerging Role in Pain Management and Health Implications.* pp 347 – 378. Hauppauge, New York: Nova Science Publishers.

Abstract:

Sundararajan, V., Taurin, S., Nimick, M., Jayawardena, N., Greish, K., and Rosengren, R.J. SMA-RL71 as a novel nanomedicine for triple negative breast cancer. *Drug Discovery and Therapy World Congress*, Boston 18 June, 2014, abstract 61.